

Correlating New Physics Effects in Semileptonic $\Delta C = 1$ and $\Delta S = 1$ Processes

Svjetlana Fajfer,^{a,b} Jernej F. Kamenik,^{a,b} Arman Korajac^b and Nejc Košnik^{a,b}

^a*Department of Physics, University of Ljubljana,
Jadranska 19, 1000 Ljubljana, Slovenia*

^b*J. Stefan Institute,
Jamova 39, P. O. Box 3000, 1001 Ljubljana, Slovenia*

E-mail: svjetlana.fajfer@ijs.si, jernef.kamenik@cern.ch,
arman.korajac@ijs.si, nejc.kosnik@ijs.si

ABSTRACT: We present constraints on the left-handed dimension-6 interactions that contribute to semileptonic and leptonic decays of K , D , pions and to nuclear beta decay. We employ the flavour covariant description of the effective couplings, identify universal CP phases of New Physics and derive constraints from decay rates and CP-odd quantities. As a result, we can predict the maximal effects of such flavoured NP in D decays from stringent K decay constraints and vice-versa.

KEYWORDS: Charm Flavour Violation, Kaons, CP Violation, SMEFT

ARXIV EPRINT: [2305.13851](https://arxiv.org/abs/2305.13851)

Contents

1	Introduction	1
2	Framework	3
3	Aligning BSM flavour structures with $\Delta S = 1$ and $\Delta C = 1$ constraints	5
3.1	Matching to weak effective theory	6
4	$s \rightarrow d\nu\bar{\nu}$ and $c \rightarrow u\ell^+\ell^-$	7
4.1	$K^+ \rightarrow \pi^+\nu\bar{\nu}$ and $K_L \rightarrow \pi^0\nu\bar{\nu}$	8
4.2	$D^0 \rightarrow \ell^+\ell^-$ and $D^+ \rightarrow \pi^+\ell^+\ell^-$	9
5	$s \rightarrow d\ell^+\ell^-$ and $c \rightarrow u\nu\bar{\nu}$	11
5.1	$K_L \rightarrow \pi^0\ell^+\ell^-$ and $K_L \rightarrow \ell^+\ell^-$	11
5.2	$K_L \rightarrow \ell^+\ell^-$	12
5.3	$D^0 \rightarrow \pi^0\nu\bar{\nu}$	13
6	High-p_T limits	13
7	Charged currents at low energies and at high-p_T	14
8	Results	15
9	Conclusions	16
A	Lepton-specific CKM elements	21
A.1	V_{ud}^ℓ	21
A.2	V_{us}^ℓ	22
A.3	V_{cd}^ℓ and V_{cs}^ℓ	22
A.4	Limits	22

1 Introduction

The Standard Model (SM) has a unique way of incorporating CP violation (CPV) and suppressing flavour changing neutral currents (FCNCs) in the quark sector. In particular, the lightness of the first two generations and the suppressed mixing with the third generation severely suppress FCNC transitions involving only the first two generation quarks. This is manifest in particular in processes which are characterized by so called hard GIM, such as those involving CPV. In fact, no significant deviations from the SM predictions related to strangeness (S) and charm (C) flavour violation have been observed in experiments to date, placing stringent limits on possible beyond the SM (BSM) effects in these sectors.

On the other hand, observed hints of deviations from SM predictions in semileptonic $\Delta B = 1$ processes (both in $b \rightarrow s\mu\mu$ FCNCs and in particular in $b \rightarrow c\tau\nu$ charged current (CC) mediated semileptonic b -hadron decays), still await experimental clarification, and have triggered many studies throughout the last decade (see e.g. refs. [1, 2]). Intriguingly, the most straightforward and successful BSM proposals addressing the $\Delta B = 1$ FCNC and CC observables introduce new interactions of left-handed quarks (and leptons) [3–10], which imply novel flavour breaking sources (besides SM Yukawas) of the $U(3)_Q$ flavour symmetry, respected by the SM gauge interactions. This already motivated a reconsideration of BSM effects in (rare) (semi)leptonic decays of kaons [11, 12], D -mesons [13–17], B -mesons [18] and also top quarks [19].

Experimentally, there has been recent progress in the search for rare $\Delta C = 1$ leptonic $D^0 \rightarrow \mu^+\mu^-$ [20] decay as well as the analysis of non-resonant regions of the differential rate for $D^+ \rightarrow \pi^+\mu^+\mu^-$ [21] by the LHCb collaboration. BESIII collaboration has also recently reported results from a first dedicated search for $D^0 \rightarrow \pi^0\nu\bar{\nu}$ decay [22]. Similarly, new results have been recently reported on semileptonic $\Delta S = 1$ transitions in both charged [23, 24] and neutral [25] kaon decays by the NA62 and KOTO collaborations, respectively. Further significant improvements in these measurements and searches are expected from these and the next generation of flavour experiments [26].

Motivated by these developments, we investigate the interplay of possible NP effects in semileptonic CC and FCNC transitions involving purely left-handed first- and second-generation quarks. In particular, it has been shown previously [27] that the peculiar structure of $U(3)_Q$ breaking in the SM implies that possible BSM sources of CPV in this sector affect rare charm and kaon decays in a universal way (see also ref. [28]). We demonstrate how and when existing bounds on CPV in rare semileptonic K meson decays severely constrain the possible size of the corresponding effects in charm decays, and vice-versa. Employing the covariant parametrization of flavour conversion developed in refs. [28–30] we constrain the unique new CPV parameter whose effect cannot be tuned by adjusting the alignment angle of BSM flavour breaking to down-quark or up-quark basis. Furthermore, we derive robust model-independent bounds on BSM affecting either charm or kaon semileptonic decays, and discuss the interplay between CC and FCNC transitions. Finally, we study the increasingly important constraints posed by the experimental studies of high- p_T semileptonic processes at the LHC $pp \rightarrow \ell\nu(\ell^+\ell^-)$ [31–33].

The remainder of the paper is structured as follows: in section 2 we review the basic elements of the SM effective theory (SMEFT) of flavour conversion including CPV within the first two generations of left-handed quarks. We apply this framework to (rare) semileptonic K and D meson decays in section 3. Sections 4 and 5 contain the detailed discussion of the relevant observables connecting and constraining the semileptonic $\Delta C = 1$ and $\Delta S = 1$ FCNC processes $s \rightarrow d\nu\bar{\nu}$ and $c \rightarrow u\ell^+\ell^-$, and $s \rightarrow d\ell^+\ell^-$ and $c \rightarrow u\nu\bar{\nu}$, respectively. We explain the interplay between the two sectors in high- p_T collider experiments in section 6 and discuss the additional correlations introduced by the inclusion of CC processes in section 7. Section 8 contains our main results and projections, while we present our conclusions and prospects for future experiments in section 9.

2 Framework

We are interested in BSM effects in semileptonic transitions involving exclusively left-handed quarks of first two generations. Working within the SM effective field theory (SMEFT) [34] valid below a heavy new physics (NP) threshold scale Λ , we thus supplement the SM Lagrangian by local semileptonic effective operators with left-chiral quarks¹

$$\mathcal{L}_{\text{SMEFT}} \supset \frac{X_{ij}^{(3,\ell)}}{\Lambda^2} (\bar{Q}_i \gamma_\mu \sigma^a Q_j) (\bar{L}_\ell \gamma^\mu \sigma_a L_\ell) + \frac{X_{ij}^{(1,\ell)}}{\Lambda^2} (\bar{Q}_i \gamma_\mu Q_j) (\bar{L}_\ell \gamma^\mu L_\ell). \quad (2.1)$$

Here Q_i is the i -th generation left-handed quark doublet, which we write in the down-quark mass basis as $Q_i = (u'_{Li}, d_{Li})^T$. The up-quark fields in this basis are related to their mass eigenstates via the CKM matrix V as $u'_i = V_{ji}^* u_j$. For leptons we choose the charged lepton mass basis: $L_i = (U_{ji}^* \nu_{Lj}, \ell_{Li})^T$, where U is the PMNS matrix. Pauli matrices σ^a , $a = 1, 2, 3$, act in the $SU(2)_L$ space. We assume in eq. (2.1) that lepton flavour is conserved, whereas the BSM quark flavour conversion is parametrized by Hermitian matrices $X^{(1,\ell)}, X^{(3,\ell)}$. The resulting Lagrangian containing FCNCs reads

$$\begin{aligned} \mathcal{L}_{\text{FCNC}} = & \frac{1}{\Lambda^2} X_{ij}^{(+)} \left[(\bar{u}'_i \gamma^\mu P_L u'_j) (\bar{\nu} \gamma_\mu P_L \nu) + (\bar{d}'_i \gamma^\mu P_L d_j) (\bar{\ell} \gamma_\mu P_L \ell) \right] \\ & + \frac{1}{\Lambda^2} X_{ij}^{(-)} \left[(\bar{u}'_i \gamma^\mu P_L u'_j) (\bar{\ell} \gamma_\mu P_L \ell) + (\bar{d}'_i \gamma^\mu P_L d_j) (\bar{\nu} \gamma_\mu P_L \nu) \right], \end{aligned} \quad (2.2)$$

where $P_{R,L} = (1 \pm \gamma_5)/2$. Above, we have introduced the matrices $X^{(\pm)} = X^{(1)} \pm X^{(3)}$ and suppressed explicit lepton flavour index for clarity. On the other hand, the charged currents stemming from eq. (2.1) are only due to the $X^{(3)}$

$$\mathcal{L}_{\text{CC}} = \frac{1}{\Lambda^2} 2X_{ij}^{(3)} (\bar{u}'_i \gamma^\mu P_L d_j) (\bar{\ell} \gamma_\mu P_L \nu) + \text{h.c.} \quad (2.3)$$

Next we focus exclusively on the first two generations and use the fact that any two-dimensional hermitian matrix can be decomposed in terms of the identity and Pauli matrices. Note that in isolating the first two generations in the following we are neglecting possible additional BSM effects due to mixing with the third quark generation. However, the resulting modifications of our results are in general severely suppressed due the hierarchical structure of the SM quark Yukawas. See ref. [27] for in depth discussion on this point. We can write

$$X_{ij}^{(\pm)} = \lambda^{(\pm)} \delta_{ij} + c_a^{(\pm)} (\sigma^a)_{ij}, \quad (2.4)$$

where λ and c_a are real. It is only the traceless part (c_a) that plays a role in FCNC processes. In contrast, λ 's contribute to flavour-diagonal neutral currents as well as to charged current processes via $X^{(3)}$:

$$2X_{ij}^{(3)} = (\lambda^{(+)} - \lambda^{(-)}) \delta_{ij} + (c_a^{(+)} - c_a^{(-)}) (\sigma^a)_{ij}. \quad (2.5)$$

¹Additional SMEFT operators modifying W and Z couplings can also modify semileptonic processes and are constrained by precision measurements of on-shell massive weak vector bosons at LEP [35–37]. For analysis of NP in W/Z couplings to fermions see [38–41].

Notice that a unique parameter, $c_2^{(\pm)}$, encodes CP violation, while the remaining three couplings are real. The traceless part of the coupling matrix offers an intuitive geometrical interpretation [30] since it spans a 3-dimensional space. Each traceless hermitian matrix A is equivalent to a real 3-dimensional vector \mathbf{a} via the mapping $A = \mathbf{a} \cdot \boldsymbol{\sigma}$. Scalar and cross product between vectors \mathbf{a}, \mathbf{b} (corresponding to matrices $A = \mathbf{a} \cdot \boldsymbol{\sigma}, B = \mathbf{b} \cdot \boldsymbol{\sigma}$) are defined via matrix operations as

$$\mathbf{a} \cdot \mathbf{b} \equiv \frac{1}{2} \text{Tr}[AB], \quad \mathbf{a} \times \mathbf{b} \equiv \frac{-i}{2} [A, B], \quad (2.6)$$

and allow for interpretation in terms of lengths, angles and volumes.

Our analysis is based on the SM flavour group for the first two quark generations $\mathcal{F} = \text{U}(2)_Q \times \text{U}(2)_U \times \text{U}(2)_D$ where Q, U and D stand for quarks doublets, up-type singlets and down-type singlets, respectively [28, 30]. The group \mathcal{F} is broken within the SM only by the Yukawa interactions. To better understand the resulting pattern of flavour and CP violation in and beyond the SM, we promote Y_u and Y_d to spurions that transform under \mathcal{F} as $(2, 2, 1)$ and $(2, 1, 2)$, respectively. In order to construct \mathcal{F} -invariant terms we furthermore define the spurions $Y_u Y_u^\dagger$ and $Y_d Y_d^\dagger$. They belong to the $(3 \oplus 1, 1, 1)$ representation of \mathcal{F} . Since the traces of these matrices do not affect flavour-changing processes, it is useful to remove them and work with traceless parts:

$$\mathcal{A}_{u,d} = (Y_{u,d} Y_{u,d}^\dagger)_{\psi\psi}, \quad \text{where } M_{\psi\psi} \equiv M - \frac{1}{2} \mathbb{I} \text{tr} M. \quad (2.7)$$

Both $\mathcal{A}_{u,d}$ belong to the adjoint representation of $\text{U}(2)_Q$. Without loss of generality, we can choose to work in a basis with diagonal down-quark Yukawa couplings, $Y_d = \text{diag}(y_d, y_s)$, whereas $Y_u = V_{\text{CKM}} \text{diag}(y_u, y_c)$. There is no CP violation in the SM with two generations, leading to V_{CKM} being just a rotation matrix with the Cabibbo angle θ_c . Inserting Y_u and Y_d , we get:

$$\mathcal{A}_d = \frac{y_d^2 - y_s^2}{2} \sigma_3, \quad (2.8)$$

$$\mathcal{A}_u = V \begin{pmatrix} y_u & 0 \\ 0 & y_c \end{pmatrix}^2 V^T = \frac{y_c^2 - y_u^2}{2} \left(-\cos(2\theta_c) \sigma_3 + \sin(2\theta_c) \sigma_1 \right). \quad (2.9)$$

For later convenience, we introduce normalised vectors

$$\hat{\mathcal{A}}_d = -\sigma_3, \quad (2.10)$$

$$\hat{\mathcal{A}}_u = -\cos(2\theta_c) \sigma_3 + \sin(2\theta_c) \sigma_1, \quad (2.11)$$

which are shown in figure 1. These two basis vectors present two special directions in the coupling space of X , since alignment of X along one of them, $X \propto \mathcal{A}_{u,d}$, implies no FCNCs in up-type or down-type quarks, respectively. However, BSM couplings can also span the orthogonal direction along σ_2 . The most general form of X that includes this CPV direction can thus be written as $X_{\psi\psi} = \alpha \hat{\mathcal{A}}_u + \beta \hat{\mathcal{A}}_d + i\gamma [\hat{\mathcal{A}}_u, \hat{\mathcal{A}}_d]$. In the remainder of this paper, we shall use cylindrical coordinates c_R, c_I , and θ_d , which are related to the

cartesian ones as $c_1 = c_R \sin \theta_d$, $c_3 = -c_R \cos \theta_d$ and $c_2 = c_I$. The most general form of X then reads

$$X = \lambda \mathbb{1} + c_R \sin \theta_d \sigma_1 + c_I \sigma_2 - c_R \cos \theta_d \sigma_3. \quad (2.12)$$

We conclude this section by commenting on the approximations taken in the two generation limit of the SM. Within the full three-generation SM (as well as in minimally flavour violating (MFV) NP scenarios [42]) CPV effects in flavour changing processes among the first two generations are not strictly vanishing, but are nonetheless severely suppressed by small CKM mixing with the third generation. Within our framework, such suppressed effects would lead to $\mathcal{A}_{u,d}$ acquiring small components in the σ_2 direction in flavour space. The NP flavour alignment limit with either up- or down-type quark mass basis would then imply alignment of NP and SM CPV phases as well. In our analysis we are neglecting these subleading, suppressed CPV effects of NP and are thus effectively probing (CPV) NP effects beyond MFV.

3 Aligning BSM flavour structures with $\Delta S = 1$ and $\Delta C = 1$ constraints

We first focus on the allowed size of the CP-even c_R and CP-odd c_I couplings depending on the alignment angle θ_d . At low energies, the $X^{(\pm)}$ matrices map onto parameters of the effective Lagrangian

$$\begin{aligned} \mathcal{L}_{\text{eff}}^{(\pm)} = & \frac{z_{\Delta S=1}^{(-)}}{\Lambda^2} (\bar{d}_L \gamma^\mu s_L) (\bar{\nu}_L \gamma_\mu \nu_L) + \frac{z_{\Delta C=1}^{(-)}}{\Lambda^2} (\bar{u}_L \gamma^\mu c_L) (\bar{\ell}_L \gamma_\mu \ell_L) + \\ & + \frac{z_{\Delta S=1}^{(+)}}{\Lambda^2} (\bar{d}_L \gamma^\mu s_L) (\bar{\ell}_L \gamma_\mu \ell_L) + \frac{z_{\Delta C=1}^{(+)}}{\Lambda^2} (\bar{u}_L \gamma^\mu c_L) (\bar{\nu}_L \gamma_\mu \nu_L) + \text{h.c.}, \end{aligned} \quad (3.1)$$

written in the fermion mass basis. The magnitudes $|z_{\Delta S=1}^{(\pm)}|$, $|z_{\Delta C=1}^{(\pm)}|$ can be geometrically expressed in a manifestly basis-independent form:

$$|z_{\Delta S=1}^{(\pm)}| = |X^{(\pm)} \times \hat{\mathcal{A}}_d| = \sqrt{(c_R^{(\pm)} \sin \theta_d^{(\pm)})^2 + (c_I^{(\pm)})^2}, \quad (3.2)$$

$$|z_{\Delta C=1}^{(\pm)}| = |X^{(\pm)} \times \hat{\mathcal{A}}_u| = \sqrt{(c_R^{(\pm)} \sin(2\theta_c - \theta_d^{(\pm)}))^2 + (c_I^{(\pm)})^2}. \quad (3.3)$$

For $|z_{\Delta S=1}^{(\pm)}|$, the above form can be understood in the down-quark basis where $\hat{\mathcal{A}}_d$ is proportional to σ_3 . Then, $z_{\Delta S=1}^{(\pm)}$ corresponds to $X_{12}^{(\pm)}$, whose size is given by $\sqrt{(c_R \sin \theta_d)^2 + c_I^2}|_{(\pm)}$. This is exactly the length of the orthogonal component of $X^{(\pm)}$ to $\hat{\mathcal{A}}_d$ obtained by the cross-product [30]. The analogous argument holds for $|z_{\Delta C=1}^{(\pm)}|$ when we analyse it in the up-quark mass basis. On the other hand, the CP-violating imaginary part is universal since it is normal to the $\hat{\mathcal{A}}_d - \hat{\mathcal{A}}_u$ plane and thus insensitive to rotations in the 1 – 3 plane:

$$\Im(z_{\Delta S=1}^{(\pm)}) = \Im(z_{\Delta C=1}^{(\pm)}) = \Im\left(X^{(\pm)} \cdot \frac{\hat{\mathcal{A}}_d \times \hat{\mathcal{A}}_u}{|\hat{\mathcal{A}}_d \times \hat{\mathcal{A}}_u|}\right) = c_I^{(\pm)}. \quad (3.4)$$

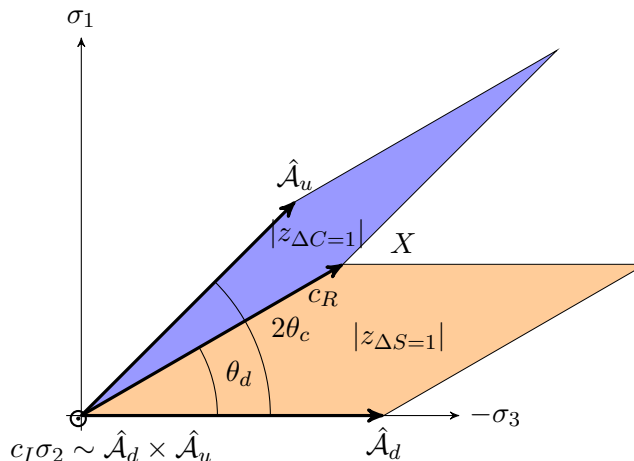


Figure 1. Schematic of possible NP contributions to $\Delta S = 1$ and $\Delta C = 1$ FCNC semileptonic processes in the two-generation limit of SM. CP conserving magnitudes of NP contributions ($|z_{\Delta C=1}|, |z_{\Delta S=1}|$) depend on the alignment angle θ_d . CPV NP contributions (c_I) are independent of θ_d . See text for details.

If we rely only on the CP-even experimental upper bounds, namely if we know only upper bounds $|z_{\Delta S=1}^{\text{exp}}|$ and $|z_{\Delta C=1}^{\text{exp}}|$, we can minimise the effect in rare kaon decays when θ_d is small since X , in this case, is aligned towards the down-quark mass basis. Conversely, we get a minimal effect in D meson decays at an angle $\theta_d = 2\theta_c$. At small θ_d (down-alignment) we thus expect $\Delta C = 1$ constraints to dominate, whereas for $\theta_d \approx 2\theta_c$ (up-alignment) the $\Delta S = 1$ processes become more important. In between the two regimes lies an optimal value of angle θ_d^* at which the constraints on $|X|$ stemming from $|z_{\Delta S=1}^{\text{exp}}|$ and $|z_{\Delta C=1}^{\text{exp}}|$ coincide numerically, i.e. when $|z_{\Delta S=1}/z_{\Delta C=1}| = |z_{\Delta S=1}^{\text{exp}}/z_{\Delta C=1}^{\text{exp}}| \equiv r_{\text{exp}}$. Assuming that the alignment angle is in the range $0 \leq \theta_d \leq 2\theta_c$, we find

$$\tan \theta_d^* = \frac{c_R^2 r_{\text{exp}}^2 \sin(4\theta_c)/\sqrt{2} - \sqrt{-2c_I^2(c_I^2 + c_R^2) (r_{\text{exp}}^2 - 1)^2 + 2r_{\text{exp}}^2 c_R^4 \sin^2 2\theta_c}}{\sqrt{2} [c_I^2 (r_{\text{exp}}^2 - 1) + c_R^2 r_{\text{exp}}^2 \cos^2(2\theta_c) - c_R^2]} \quad (3.5)$$

In the regime of large CPV, $|c_I| \gg c_R$, there is no solution for θ_d^* , since the effect of θ_d is rendered unimportant. The optimal alignment in the CP-conserving limit with $c_I = 0$ reads

$$\tan \theta_d^*|_{c_I=0} = \frac{r_{\text{exp}} \sin 2\theta_c}{1 + r_{\text{exp}} \cos 2\theta_c} \quad (3.6)$$

3.1 Matching to weak effective theory

At low energies, we rely on the weak effective theory (WET) and use standard conventions for the Hamiltonian governing $\Delta C = 1$ transitions

$$\mathcal{H}_{\text{eff}}^{\Delta C=1} = -\frac{4G_F}{\sqrt{2}} \frac{\alpha_{\text{em}}}{4\pi} \left(\sum_{i=9,10} C_{i,\ell}^{\Delta C=1} O_{i,\ell}^{\Delta C=1} + C_{L,\nu\ell}^{\Delta C=1} O_{L,\nu\ell}^{\Delta C=1} \right) + \text{h.c.}, \quad (3.7)$$

where the SMEFT NP effects are imprinted upon the following set of dimension-6 operators:

$$O_{9,\ell}^{\Delta C=1} = (\bar{u}\gamma_\mu P_L c)(\bar{\ell}\gamma^\mu \ell), \quad O_{L,\nu_\ell}^{\Delta C=1} = (\bar{u}\gamma_\mu P_L c)(\bar{\nu}_\ell\gamma_\mu P_L \nu_\ell), \quad (3.8)$$

$$O_{10,\ell}^{\Delta C=1} = (\bar{u}\gamma_\mu P_L c)(\bar{\ell}\gamma^\mu \gamma_5 \ell). \quad (3.9)$$

For $\Delta S = 1$ transitions, we conversely employ

$$\mathcal{H}_{\text{eff}}^{\Delta S=1} = -\frac{4G_F}{\sqrt{2}} \frac{\alpha_{\text{em}}}{4\pi} \left(\sum_{i=9,10} C_{i,\ell}^{\Delta S=1} O_{i,\ell}^{\Delta S=1} + C_{L,\ell}^{\Delta S=1} O_{L,\nu_\ell}^{\Delta S=1} \right) + \text{h.c.} \quad (3.10)$$

The operators for the down-quark sector have the same structure as those for the up-quark sector; they differ in a simple replacements of $u \rightarrow d$ and $c \rightarrow s$. Here, $\ell = e, \mu$ or τ . We will separate the contribution of SM and NP to the Wilson coefficients:

$$C_i = C_i^{\text{SM}} + C_i^{\text{NP}}. \quad (3.11)$$

The left-handed SMEFT operator structure that we consider in eq. (2.2) results in the relation $C_9^{\text{NP}} = -C_{10}^{\text{NP}}$ for charged-lepton operators. After matching $X^{(-)}$ SMEFT coefficients onto the WET Wilson coefficients, we find

$$s \rightarrow d\nu\bar{\nu} : \quad C_{L,\nu}^{\Delta S=1,\text{NP}} = \frac{2\pi}{\alpha_{\text{em}}} \frac{v^2}{\Lambda^2} \left\{ c_R^{(-)} \sin\theta_d^{(-)} - ic_I^{(-)} \right\}, \quad (3.12)$$

$$c \rightarrow u\ell^+\ell^- : \quad C_9^{\Delta C=1,\text{NP}} = -C_{10}^{\Delta C=1,\text{NP}} = \frac{\pi}{\alpha_{\text{em}}} \frac{v^2}{\Lambda^2} \left\{ c_R^{(-)} \sin(\theta_d^{(-)} - 2\theta_c) - ic_I^{(-)} \right\}, \quad (3.13)$$

whereas the low-energy coefficients from $X^{(+)}$ are

$$s \rightarrow d\ell^+\ell^- : \quad C_9^{\Delta S=1,\text{NP}} = -C_{10}^{\Delta S=1,\text{NP}} = \frac{\pi}{\alpha_{\text{em}}} \frac{v^2}{\Lambda^2} \left\{ c_R^{(+)} \sin\theta_d^{(+)} - ic_I^{(+)} \right\}, \quad (3.14)$$

$$c \rightarrow u\nu\bar{\nu} : \quad C_{L,\nu}^{\Delta C=1,\text{NP}} = \frac{2\pi}{\alpha_{\text{em}}} \frac{v^2}{\Lambda^2} \left\{ c_R^{(+)} \sin(\theta_d^{(+)} - 2\theta_c) - ic_I^{(+)} \right\}. \quad (3.15)$$

The presented Wilson coefficients indicate how the CP conserving NP contributions to charm and kaon physics are related via the Cabibbo rotation and its interplay with the alignment angle. In the remainder of the paper we study current constraints on $X^{(+)}$ and $X^{(-)}$, as parameterised by $c_R^{(\pm)}$, $\theta_d^{(\pm)}$ and $c_I^{(\pm)}$. The presence of $c_I^{(\pm)}$ without any θ_d dependence implies the flavour universal character of the CPV parameters.

In our numerical studies we set the scale to $\Lambda = 1$ TeV, thus all the presented bounds on $c_{R,I}$ should be understood as bounds on $(\text{TeV}/\Lambda)^2 c_{R,I}(\Lambda)$.²

4 $s \rightarrow d\nu\bar{\nu}$ and $c \rightarrow u\ell^+\ell^-$

The elements of the $X^{(-)}$ matrix, parametrised by $c_R^{(-)}$, $\theta_d^{(-)}$, $c_I^{(-)}$ enter in the amplitudes for $s \rightarrow d\nu\bar{\nu}$ and $c \rightarrow u\ell^+\ell^-$ processes. The branching ratio for $K \rightarrow \pi\nu\bar{\nu}$ is rather well determined and probing the SM short-distance contribution. However, in rare charm meson

²The renormalization group running effects of the left-handed semileptonic operators are negligible [43].

Observable	Exp. constraint	Reference
$\mathcal{B}(K^+ \rightarrow \pi^+ \nu \bar{\nu})$	$(1.14^{+0.40}_{-0.33}) \times 10^{-10}$	[37] ([23, 44])
$\mathcal{B}(D^0 \rightarrow e^+ e^-)$	$< 7.9 \times 10^{-8}$	[45]
$\mathcal{B}(D^+ \rightarrow \pi^+ e^+ e^-)$	$< 1.1 \times 10^{-6}$	[21]
$\mathcal{B}(D^0 \rightarrow \mu^+ \mu^-)$	$< 3.1 \times 10^{-9}$	[20]
$\mathcal{B}(D^+ \rightarrow \pi^+ \mu^+ \mu^-)$	$< 6.7 \times 10^{-8}$	[46]
$pp \rightarrow e^+ e^-$		HighPT [47]
$pp \rightarrow \mu^+ \mu^-$		HighPT [47]
$pp \rightarrow \tau^+ \tau^-$		HighPT [47]

Table 1. Experimental constraints employed as constraints on $X^{(-)}$ couplings. Upper bounds are given at 90% CL.

decays proceeding via $c \rightarrow u \ell^+ \ell^-$ transition, the sensitivity to short distance SM contributions is reduced due to effective GIM mechanism. In addition, the larger phase space available in D meson decays leads to large long-distance contributions due intermediate kaon and pion rescattering effects. The ensuing bounds on $z_{\Delta C=1}^{(-)}$ are thus comparably not as constraining as the ones on $z_{\Delta S=1}^{(-)}$ from $s \rightarrow d \nu \bar{\nu}$. The optimal alignment angle $\theta_d^{(-)*}$ is expected to be small. In table 1 we list the relevant experimental inputs for $X^{(-)}$.

4.1 $K^+ \rightarrow \pi^+ \nu \bar{\nu}$ and $K_L \rightarrow \pi^0 \nu \bar{\nu}$

The differential branching ratio for $K^\pm \rightarrow \pi^\pm \nu \bar{\nu}$ can be written as

$$\frac{d\mathcal{B}}{dq^2}(K^\pm \rightarrow \pi^\pm \nu \bar{\nu}) = (1 + \Delta_{\text{EM}}) \frac{G_F^2 \alpha_{\text{em}}^2}{3072 \pi^5 m_K^3 \Gamma_{K^\pm}} \lambda^{3/2}(m_\pi^2, m_{\Delta S=1}^2, q^2) f_{+,K \rightarrow \pi}^2(q^2) |C_{L,\nu}^{\Delta S=1}|^2, \quad (4.1)$$

where the Wilson coefficient C_{L,ν_ℓ} contains the SM short-distance contribution as well as the contribution of $X^{(-)}$

$$C_{L,\nu}^{\Delta S=1} = C_{L,\nu}^{\Delta S=1,\text{SM}} + C_{L,\nu_\ell}^{\Delta S=1,\text{NP}} = \frac{2(\lambda_c X_c^\ell + \lambda_t X_t)}{\sin^2 \theta_w} + \frac{2\pi v^2}{\alpha_{\text{em}} \Lambda^2} \left(c_R^{(-)} \sin \theta_d^{(-)} - i c_I^{(-)} \right). \quad (4.2)$$

The SM contributions have been carefully analysed by several authors [48–52]. Here, $\lambda_q = V_{qs}^* V_{qd}$, X_t denotes the virtual top-quark contribution, and X_c the charm-quark contribution. The electromagnetic correction $\Delta_{\text{EM}} \simeq -0.3\%$ was calculated in ref. [53]. The charm contribution has a mild sensitivity to the lepton flavour, and we take the following values for the Inami-Lim functions

$$X_t = 1.464(17), \quad X_c^e \simeq X_c^\mu = 1.04(3) \times 10^{-3}, \quad X_c^\tau = 0.70(2) \times 10^{-3}. \quad (4.3)$$

The uncertainty of X_t has been estimated in refs. [49, 54, 55], whereas the uncertainty of X_c was recently discussed in ref. [48]. For the $K \rightarrow \pi$ form factors, we employ lattice

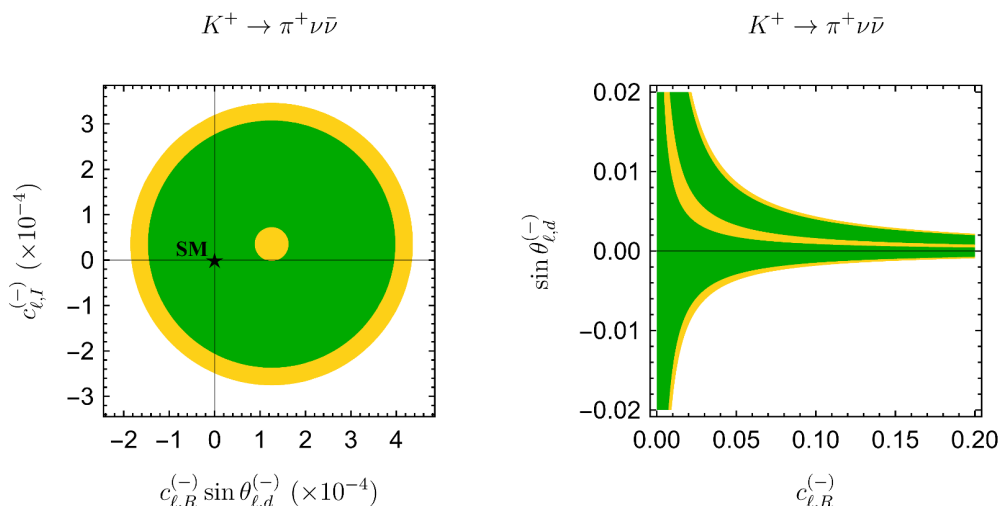


Figure 2. Left: constraints in the plane of $c_{\ell,R}^{(-)} \sin \theta_{\ell,d}^{(-)}$ and $c_{\ell,I}^{(-)}$ due to the measured $\mathcal{B}(K^+ \rightarrow \pi^+ \nu \bar{\nu})$. These constraints are valid for any lepton flavour $\ell = e, \mu, \tau$. Right: weakest constraints in the plane of $c_{\ell,R}^{(-)}$ and $\sin \theta_{\ell,d}^{(-)}$, which occur for $c_{\ell,I}^{(-)} \simeq 0.4 \times 10^{-4}$.

results [56]. We neglect long-distance contributions since it has been shown that they are subleading in this decay [57, 58]. Current experimental bound on this process is driven by the NA62 measurement [23], whereas the world average is $\mathcal{B}(K^+ \rightarrow \pi^+ \nu \bar{\nu}) = (1.14_{-0.33}^{+0.40}) \times 10^{-10}$ [37].

On the other hand, the amplitude for the $K_L \rightarrow \pi^0 \nu \bar{\nu}$ decay is sensitive exclusively to CP-odd effects, leading to the branching fraction

$$\frac{d\mathcal{B}}{dq^2}(K_L \rightarrow \pi^0 \nu \bar{\nu}) = \frac{G_F^2 \alpha_{\text{em}}^2}{1536 \pi^5 m_K^3 \Gamma_{K_L}} \lambda^{3/2}(m_\pi^2, m_K^2, q^2) f_{+,K \rightarrow \pi}^2(q^2) \left[\Im(C_{L,\nu}^{\Delta S=1}) \right]^2, \quad (4.4)$$

where

$$\Im(C_{L,\nu}^{\Delta S=1}) = \frac{2 X_t \text{Im} \lambda_t}{\sin^2 \theta_w} - \frac{2\pi v^2}{\alpha_{\text{em}} \Lambda^2} c_{I,\nu}^{(-)}. \quad (4.5)$$

Using the current 90% C.L. experimental bound $\mathcal{B}(K_L \rightarrow \pi^0 \nu \bar{\nu}) < 3.0 \times 10^{-9}$ [59], we derive the constraint $-6.3 \times 10^{-4} < c_{\ell,I}^{(-)} < 5.6 \times 10^{-4}$, for all ℓ , which is weaker than the corresponding bound one obtains from $K^+ \rightarrow \pi^+ \nu \bar{\nu}$ (see figure 2)

$$-2.8 \times 10^{-4} < c_{\ell,I}^{(-)} < 3.5 \times 10^{-4}. \quad (4.6)$$

Note that the bounds on $c_{\tau,I}^{(-)}$ differ minutely due to m_τ effects in the loops.

4.2 $D^0 \rightarrow \ell^+ \ell^-$ and $D^+ \rightarrow \pi^+ \ell^+ \ell^-$

In the SM, the branching ratio for $D^0 \rightarrow \mu^+ \mu^-$ is dominated by long-distance contributions of the $D^0 \rightarrow \gamma^* \gamma^*$ intermediate state. However, the relation $\mathcal{B}(D^0 \rightarrow \mu^+ \mu^-) \approx 2.7 \times 10^{-5} \times$

$\mathcal{B}(D^0 \rightarrow \gamma\gamma)$ [60] and the upper bound $\mathcal{B}(D^0 \rightarrow \gamma\gamma) < 8.5 \times 10^{-7}$ [61] guarantee that the SM long-distance branching fraction is $\lesssim 10^{-11}$, far below the current experimental upper bound, $\mathcal{B}(D^0 \rightarrow \mu^+\mu^-) < 3.1 \times 10^{-9}$ [20]. Similar conclusion also holds for $D^0 \rightarrow e^+e^-$ [60, 62]. The short-distance contribution to the branching ratio is given by [13]

$$\mathcal{B}(D^0 \rightarrow \ell^+\ell^-) = \frac{G_F^2 \alpha_{\text{em}}^2}{16\pi^3 \Gamma_{D^0}} m_D m_\ell^2 f_D^2 \sqrt{1 - 4m_\ell^2/m_D^2} |C_{10}^{\Delta C=1}|^2, \quad (4.7)$$

where we can safely neglect SM contributions to $C_{10}^{\Delta C=1}$. On the other hand, the differential branching ratio of $D \rightarrow \pi\ell^+\ell^-$ is sensitive to both vector $C_9^{\Delta C=1}$ and axial $C_{10}^{\Delta C=1}$ Wilson coefficients

$$\frac{d\mathcal{B}}{dq^2}(D^+ \rightarrow \pi^+\ell^+\ell^-) = \frac{G_F^2 \alpha_{\text{em}}^2}{1536\pi^5 m_D^3 \Gamma_{D^0}} \lambda^{1/2}(m_\pi^2, m_D^2, q^2) \sqrt{1 - 4m_\ell^2/q^2} \left(\mathcal{I}_V^D(q^2) + \mathcal{I}_A^D(q^2) \right), \quad (4.8)$$

where axial and vector lepton current contributions are

$$\begin{aligned} \mathcal{I}_A^D(q^2) &= |C_{10}^{\Delta C=1}|^2 \left(f_+^2(q^2) \lambda(q^2, m_D^2, m_\pi^2) \left(1 - \frac{4m_\ell^2}{q^2} \right) + 6 \frac{m_\ell^2}{q^2} (m_D^2 - m_\pi^2)^2 f_0^2(q^2) \right), \\ \mathcal{I}_V^D(q^2) &= |C_9^{\Delta C=1}|^2 f_+^2(q^2) \lambda(q^2, m_D^2, m_\pi^2) \left(1 + \frac{2m_\ell^2}{q^2} \right) + \dots, \end{aligned} \quad (4.9)$$

and $\lambda(x, y, z) = (x + y + z)^2 - 4(xy + yz + zx)$. Our results coincide with the ones given in ref. [53]. The expression (4.8) can be employed also for $D^0 \rightarrow \pi^0\ell^+\ell^-$ albeit with an additional factor 1/2. The limit extraction on short-distance NP for $D^+ \rightarrow \pi^+\ell^+\ell^-$ is more complicated due to diverse resonant long-distance contributions (indicated by ellipsis in eq. (4.9)). One solution is to integrate over the high- q^2 phase-space portion which is free of those contributions (if appropriate bounds exist, like e.g. for $D^+ \rightarrow \pi^+\mu^+\mu^-$ [46]), or integrating over the whole kinematic region together with parametrizing the dominant long-distance contributions in terms of Breit-Wigner resonances [63]. A careful analysis taking the latter approach was done in ref. [31], from where we take the resulting limits on $|C_{9,10}^{\Delta C=1}|$.

We have checked that the limit from $D^0 \rightarrow \mu^+\mu^-$ branching fraction is stronger than the one coming from $D^+ \rightarrow \pi^+\mu^+\mu^-$, whereas the opposite is true for modes with electrons. Explicitly, in the case of muons, they read

$$\left| c_{\mu,R}^{(-)} \sin(\theta_{\mu,d}^{(-)} - 2\theta_c) - i c_{\mu,I}^{(-)} \right| < 2.4 \times 10^{-2}. \quad (4.10)$$

Due to the limits coming from the branching ratio for $K^+ \rightarrow \pi^+\nu\bar{\nu}$ that are $\sim 10^{-4}$ for both $c_I^{(-)}$ and $c_R^{(-)} \sin \theta_d^{(-)}$, see figure 2, we can simplify eq. (4.10) as

$$\left| c_{\mu,R}^{(-)} \cos \theta_{\mu,d}^{(-)} \right| < \frac{2.4 \times 10^{-2}}{\sin 2\theta_c} = 0.055. \quad (4.11)$$

Similarly, for electrons we find

$$\left| c_{e,R}^{(-)} \cos \theta_{e,d}^{(-)} \right| < 0.43. \quad (4.12)$$

Observable	Exp. constraint	Reference
$\mathcal{B}(K_L \rightarrow e^+e^-)$	$(9_{-4}^{+6}) \times 10^{-12}$	[37] ([64])
$\mathcal{B}(K_L \rightarrow \mu^+\mu^-)$	$(6.84 \pm 0.11) \times 10^{-9}$	[37] ([65])
$\mathcal{B}(K_L \rightarrow \pi^0 e^+e^-)$	$< 2.8 \times 10^{-10}$	[37]
$\mathcal{B}(K_L \rightarrow \pi^0 \mu^+\mu^-)$	$< 3.8 \times 10^{-10}$	[37] ([66])
$\mathcal{B}(D^0 \rightarrow \pi^0 \nu \bar{\nu})$	$< 2.1 \times 10^{-4}$	[22]
$pp \rightarrow e^+e^-$		HighPT [47]
$pp \rightarrow \mu^+\mu^-$		HighPT [47]
$pp \rightarrow \tau^+\tau^-$		HighPT [47]

Table 2. Experimental constraints employed as constraints on $X^{(+)}$ couplings. Upper bounds are given at 90% CL.

5 $s \rightarrow d\ell^+\ell^-$ and $c \rightarrow u\nu\bar{\nu}$

The elements of the $X^{(+)}$ matrix enter in the amplitudes for $s \rightarrow d\ell^+\ell^-$ and $c \rightarrow u\nu\bar{\nu}$ processes. In the charm sector, there exists a single bound on the branching ratio $\mathcal{B}(D \rightarrow \pi\nu\bar{\nu})$ obtained recently by BESIII, which is still well above the GIM suppressed SM prediction. In contrast there already exist numerous experimental probes of the strange sector — the branching ratios $\mathcal{B}(K_{L/S} \rightarrow \ell^+\ell^-)$, as well as semileptonic decays i.e. $K_L \rightarrow \pi^0\ell^+\ell^-$. The kaon observables with charged leptons however receive sizable long-distance non-perturbative SM contributions and thus suffer from larger theoretical uncertainties. This renders the HighPT constraints on the (+) sector to be even more important than in the case of (−) couplings. We list the relevant experimental inputs for $X^{(+)}$ in table 2.

5.1 $K_L \rightarrow \pi^0\ell^+\ell^-$ and $K_L \rightarrow \ell^+\ell^-$

The rare semileptonic decay $K_L \rightarrow \pi^0\ell^+\ell^-$ is sensitive to CP-odd short distance effects, parameterized by $c_I^{(+)}$. However, the SM amplitude is dominated by long-distance dynamics. One has contributions from indirect CPV ($K_L \rightarrow K_S$ transition followed by $K_S \rightarrow \pi^0\ell^+\ell^-$), as well as CP-conserving long-distance $K_L \rightarrow \pi^0 + 2\gamma^* \rightarrow \pi^0\ell^+\ell^-$ [67–69]. Within our framework, the short-distance contribution of NP to vector and axial-vector coefficients is of the form [70]:

$$\mathcal{B}(K_L \rightarrow \pi^0\mu^+\mu^-) = (1.09(w_{7V}^2 + 2.32w_{7A}^2) \pm 2.63w_{7V}|a_S| + 3.36|a_S|^2 + 5.2) \times 10^{-12}, \quad (5.1)$$

$$\mathcal{B}(K_L \rightarrow \pi^0e^+e^-) = (4.62(w_{7V}^2 + w_{7A}^2) \pm 11.3w_{7V}|a_S| + 14.5|a_S|^2) \times 10^{-12}, \quad (5.2)$$

with:

$$w_{7V} = y_{7V} - \frac{v^2}{2\alpha_{\text{em}}\Lambda^2 \text{Im}\lambda_t} c_I^{(+)}, \quad (5.3)$$

$$w_{7A} = y_{7A} + \frac{v^2}{2\alpha_{\text{em}}\Lambda^2 \text{Im}\lambda_t} c_I^{(+)}. \quad (5.4)$$

Here $y_{7V} = 0.735$, $y_{7A} = -0.700$ [71], $|a_S| = 1.20 \pm 0.20$ [72]. Notice the ambiguity due to the unknown sign of the interference term between w_{7V} and $|a_S|$. Experimental bounds for both lepton flavours

$$\mathcal{B}(K_L \rightarrow \pi^0 \mu^+ \mu^-) < 3.8 \times 10^{-10} [66], \quad \mathcal{B}(K_L \rightarrow \pi^0 e^+ e^-) < 2.8 \times 10^{-10} [37], \quad (5.5)$$

are given at 90% CL and are an order of magnitude above the SM prediction, as can be seen when we comparing them to the respective SM predictions:

$$\mathcal{B}(K_L \rightarrow \pi^0 \mu^+ \mu^-)_{\text{SM}} = \begin{cases} (1.41_{-0.26}^{+0.28}) \times 10^{-11} ; + \text{ sign} \\ (0.95_{-0.21}^{+0.22}) \times 10^{-11} ; - \text{ sign} \end{cases}, \quad (5.6)$$

$$\mathcal{B}(K_L \rightarrow \pi^0 e^+ e^-)_{\text{SM}} = \begin{cases} (3.54_{-0.85}^{+0.98}) \times 10^{-11} ; + \text{ sign} \\ (1.56_{-0.49}^{+0.62}) \times 10^{-11} ; - \text{ sign} \end{cases}. \quad (5.7)$$

The + and - signs correspond to the sign chosen in the interference term in eqs. (5.1) and (5.2). Since the SM prediction is an order of magnitude below the current experimental limits, we approximate the likelihood by neglecting the SM contributions in the fit. This enables us to derive directly the constraints³

$$|\text{Im}[c_{e,I}^{(+)}]| < 2 \times 10^{-4}, \quad |\text{Im}[c_{\mu,I}^{(+)}]| < 4 \times 10^{-4}. \quad (5.8)$$

5.2 $K_L \rightarrow \ell^+ \ell^-$

This decay mode is also dominated by long-distance SM contributions. We explore the information coming from the $K_L \rightarrow \mu^+ \mu^-$ and $K_L \rightarrow e^+ e^-$ decays as already considered in refs. [70, 73] (see also [74] for explicit analytic expressions). In our analysis we employ the lattice QCD result for the decay constant $\langle 0 | \bar{s} \gamma^\mu \gamma^5 d | K^0(p) \rangle = i f_K p^\mu$ with $f_K = 0.1557 \text{ GeV}$ [75]. The branching ratio is then given by

$$\mathcal{B}(K_L \rightarrow \ell^+ \ell^-) = \frac{G_F^2 \alpha_{\text{em}}^2}{8\pi^3} f_K^2 m_K m_\ell^2 \sqrt{1 - 4m_\ell^2/m_K^2} |C_{10}^{\Delta S=1}|^2, \quad (5.9)$$

where

$$\begin{aligned} C_{10}^{\Delta S=1} &= C_{10}^{\Delta S=1, \text{SM}} + C_{10}^{\Delta S=1, \text{NP}} \\ &= -2\pi \left(\text{Re}(\lambda_t y_{7A}) + \text{Re}(\lambda_c y_c) - \frac{v^2}{2\alpha_{\text{em}} \Lambda^2} c_R^{(+)} \sin \theta_d^{(+)} \right) + \frac{A_{L\gamma\gamma}^\ell}{\sin^2 \theta_W}. \end{aligned} \quad (5.10)$$

Notice that this process is sensitive only to CP conserving parameters $c_R^{(+)}$ and $\theta_d^{(+)}$. The factor of 2π comes from the different conventions for the effective Hamiltonian relative to [70]. Here, the long-distance two-photon intermediate state contribution has a relative sign ambiguity and is currently estimated as [76, 77]:

$$|A_{L\gamma\gamma}^\mu| = 1.98 \times 10^{-4} (0.71 \pm 0.15 \pm 1.0 - 5.21 i), \quad (5.11)$$

$$|A_{L\gamma\gamma}^e| = 1.98 \times 10^{-4} (31.91 \pm 0.22 \pm 1.0 - 21.61 i). \quad (5.12)$$

³In addition, we have checked explicitly using results of ref. [70], that the limits from $K_S \rightarrow \ell^+ \ell^-$ are weaker compared to $K_L \rightarrow \pi \ell \ell$.

The resulting SM predictions for the branching fractions are $\mathcal{B}(K_L \rightarrow \mu^+ \mu^-) = (7.64 \pm 0.73) \times 10^{-9}$ [73], and $\mathcal{B}(K_L \rightarrow e^+ e^-) = (9.0 \pm 0.5) \times 10^{-12}$ [78]. Both theoretical estimates are comparable to the experimentally measured values [37]:

$$\mathcal{B}(K_L \rightarrow \mu^+ \mu^-)^{\text{exp}} = (6.84 \pm 0.11) \times 10^{-9}, \quad (5.13)$$

$$\mathcal{B}(K_L \rightarrow e^+ e^-)^{\text{exp}} = 9_{-4}^{+6} \times 10^{-12}. \quad (5.14)$$

5.3 $D^0 \rightarrow \pi^0 \nu \bar{\nu}$

The differential branching fraction of this decay mode depends only on the $C_{L,\nu}^{\Delta C=1}$ coefficient:

$$\frac{d\mathcal{B}}{dq^2}(D^0 \rightarrow \pi^0 \nu \bar{\nu}) = \frac{G_F^2 \alpha_{\text{em}}^2}{3072 \pi^5 m_D^3 \Gamma_{D^0}} \lambda^{3/2}(m_\pi^2, m_D^2, q^2) f_{+,D \rightarrow \pi}^2(q^2) |C_{L,\nu}^{\Delta C=1}|^2. \quad (5.15)$$

The above expression corresponds to a final state with a specific neutrino flavour in the final state. Measurable branching fraction is obtained by summing over all three neutrino flavours [15].⁴ In our setup exactly one Wilson coefficient $C_{L,\nu}^{\text{up}}$ contains a BSM contribution, while remaining flavours are purely SM. The form factor $f_+(q^2)$ in eq. (5.15) is obtained from the form factor of charged transition $D^+ \rightarrow \pi^+$, scaling it by $1/\sqrt{2}$ due to the isospin wavefunction of the π^0 state. We employ the form factor obtained using lattice QCD [80]. On the experimental side, there is a single upper limit result due to BESIII, $\mathcal{B}(D^0 \rightarrow \pi^0 \nu \bar{\nu}) < 2.1 \times 10^{-4}$ at 90% CL [22]. This bound currently results in a relatively weak constraint that cuts away large values of $|c_{\ell,R}^{(+)} \sin(\theta_{\ell,d}^{(+)} - 2\theta_c)| \lesssim 3$. It is however not competitive with the charged current constraints from LHC high- p_T tails and measurements of CKM elements, shown in figure 4.

6 High- p_T limits

An important set of limits arise when one confronts the measured cross sections of $pp \rightarrow \ell^+ \ell^-$ at the LHC against the theoretical predictions in the SM complemented by neutral current effective interactions in eq. (2.2). Extracting the bounds from high-energy $pp \rightarrow \ell^+ \ell^-$ processes is more involved due to contributions both from the up- and down-quarks. Summing over quark flavours found in the proton, we have the following set of interactions contributing incoherently to the neutral-current cross section:

$$\begin{aligned} \sigma_{\text{high-}p_T} \supset & 2 \int_{\tau_{\text{min}}}^{\tau_{\text{max}}} d\tau \frac{\tau S_{\text{had}}}{144\pi} \times \\ & \left[\mathcal{L}_{u\bar{u}} \left(\lambda^{(-)} - c_R^{(-)} \cos(2\theta_c - \theta_d^{(-)}) + F_{\text{SM},u\bar{u}} \right)^2 + \mathcal{L}_{c\bar{c}} \left(\lambda^{(-)} + c_R^{(-)} \cos(2\theta_c - \theta_d^{(-)}) + F_{\text{SM},u\bar{u}} \right)^2 \right. \\ & + \mathcal{L}_{d\bar{d}} \left(\lambda^{(+)} - c_R^{(+)} \cos\theta_d^{(+)} + F_{\text{SM},d\bar{d}} \right)^2 + \mathcal{L}_{s\bar{s}} \left(\lambda^{(+)} + c_R^{(+)} \cos\theta_d^{(+)} + F_{\text{SM},d\bar{d}} \right)^2 \\ & \left. + (\mathcal{L}_{u\bar{c}} + \mathcal{L}_{c\bar{u}}) \left((c_R^{(-)} \sin(2\theta_c - \theta_d^{(-)}))^2 + (c_I^{(-)})^2 \right) + (\mathcal{L}_{d\bar{s}} + \mathcal{L}_{s\bar{d}}) \left((c_R^{(+)} \sin\theta_d^{(+)})^2 + (c_I^{(+)})^2 \right) \right], \end{aligned} \quad (6.1)$$

⁴For constraints stemming from $B_c \rightarrow B^+ \nu \bar{\nu}$ see [79].

together with other interactions which are unaffected by the SMEFT operators. Here, $F_{\text{SM},q\bar{q}}$ denote the corresponding SM contributions, which are due to the γ and Z s -channel processes

$$\begin{aligned} F_{\text{SM},u\bar{u}}(p^2) &= \frac{Q_u e^2}{p^2} + \frac{g_{Z,u\bar{u}} g_{Z,\ell\bar{\ell}}}{p^2 - m_Z^2 + im_Z \Gamma_Z}, \\ F_{\text{SM},d\bar{d}}(p^2) &= \frac{Q_d e^2}{p^2} + \frac{g_{Z,d\bar{d}} g_{Z,\ell\bar{\ell}}}{p^2 - m_Z^2 + im_Z \Gamma_Z}, \end{aligned} \quad (6.2)$$

where $g_{Z,f\bar{f}} = \frac{2m_Z}{v}(T_f^3 - Q_f \sin^2 \theta_W)$ are the Z couplings to the fermions [81] and $p^2 = \hat{s} = \tau s_{\text{had}}$, $\sqrt{s_{\text{had}}} = 13 \text{ TeV}$. Finally, $\mathcal{L}_{q\bar{q}}$ denotes the luminosity function

$$\mathcal{L}_{q\bar{q}} \equiv \mathcal{L}_{q\bar{q}}(\tau, \mu_F) = \int_{\tau}^1 \frac{dx}{x} f_q(x, \mu_F) f_{\bar{q}}(\tau/x, \mu_F). \quad (6.3)$$

Note that we ignore SM contributions to the FCNCs, since they are suppressed by a loop factor and GIM. The latter is very effective at high energies resulting in negligible SM effects on the cross section. We employ the HighPT package [32, 47] based on ATLAS [82] and CMS [83] measurements of $pp \rightarrow \ell\ell$, in order to find bounds from high- p_T LHC data on our SMEFT parameter space.

It is evident from eq. (6.1) that the weakest bounds on $c_R^{(-)}, \theta_d^{(-)}$ will occur if we set $c_R^{(+)} = c_I^{(+)} = 0$. Furthermore, our bounds are derived by marginalizing over the trace parameters $\lambda^{(\pm)}$. The results of the marginalization procedure can be understood in advance; $\lambda^{(+)}$ will pick up a value such that $\int d\tau \tau (\mathcal{L}_{d\bar{d}}(\lambda^{(+)}) + F_{\text{SM},d\bar{d}})^2 + \mathcal{L}_{s\bar{s}}(\lambda^{(+)}) + F_{\text{SM},d\bar{d}}^2) = 0$. On the other hand, $\lambda^{(-)}$ needs to be $\lambda^{(-)} \sim c_R^{(-)} \cos 2\theta_c$ to reduce the dominant $u\bar{u}$ contribution, however, the limit will eventually be saturated through the $c\bar{c}$, $u\bar{c}$ and $\bar{u}c$ initial states. The same arguments apply if we are interested in the weakest bounds on $c_R^{(+)}, \theta_d^{(+)}$.

The bounds in both sectors are correlated, so setting a non-zero value to $c_R^{(-)}, \theta_d^{(-)}$ will shrink the allowed space in the plus region, and vice versa. Indeed the bounds will be applied separately for the $(-)$ and the $(+)$ sector assuming that couplings (\pm) are zero when deriving bounds on (\mp) .

7 Charged currents at low energies and at high- p_T

In the previous sections we have studied $c^{(+)}$ and $c^{(-)}$ separately and independently of each other. Such approach is strictly valid only if $c^{(+)} = c^{(-)}$ and there is no further effect in charged currents, see eq. (2.3). The Lagrangian that governs the semileptonic charged-current contributions at low energies can be written as:

$$\mathcal{L}_{\text{cc}} = \frac{G_F}{\sqrt{2}} V_{ij}^{\ell} (\bar{u}_i \gamma_{\mu} (1 - \gamma_5) d_j) (\bar{\ell} \gamma^{\mu} (1 - \gamma_5) \nu_{\ell}) + \text{h.c.}, \quad (7.1)$$

where $V_{ij}^{\ell} = V_{ij} + \Delta V_{ij}^{(\ell)}$ represents the NP modified effective CKM coupling. Individual lepton-specific CKM modifications depend on $c_{R,I}^{(\pm)}, \theta_d^{(\pm)}, \theta_c$ as well as on the trace parameters λ as can be seen in eq. (A.1). These modifications are subject to strong constraints

from tree-level probes of CKM elements, such as superallowed β decays, and semileptonic K , D and τ decays. Note that we can completely remove the dependence on the trace parameter $\lambda^{(3,\ell)}$ by considering the following combinations of effective CKM elements:

$$V_{us}^\ell + V_{cd}^\ell = \frac{v^2}{\Lambda^2} \left[c_R^{(+)} \sin(\theta_c + \theta_d^{(+)}) - c_R^{(-)} \sin(\theta_c + \theta_d^{(-)}) \right], \quad (7.2a)$$

$$V_{ud}^\ell - V_{cs}^\ell = \frac{v^2}{\Lambda^2} \left[-c_R^{(+)} \cos(\theta_c + \theta_d^{(+)}) + c_R^{(-)} \cos(\theta_c + \theta_d^{(-)}) + i(c_I^{(+)} - c_I^{(-)}) \sin \theta_c \right]. \quad (7.2b)$$

In the following we omit the c_I terms since they do not interfere with the SM and their size is severely constrained by neutral current processes. By squaring and summing eqs. (7.2) we can even eliminate the dependence on the Cabibbo angle:

$$\left(V_{us}^\ell + V_{cd}^\ell \right)^2 + \left(V_{cd}^\ell - V_{cs}^\ell \right)^2 = \left(\frac{v}{\Lambda} \right)^4 \left[\left(c_R^{(+)} \right)^2 + \left(c_R^{(-)} \right)^2 - 2c_R^{(+)}c_R^{(-)} \cos(\theta_d^{(+)} - \theta_d^{(-)}) \right]. \quad (7.3)$$

For completeness we also state the remaining two combinations

$$\left(\frac{V_{us}^\ell - V_{cd}^\ell}{V_{ud}^\ell + V_{cs}^\ell} \right) = 2 \left[1 + \frac{v^2}{\Lambda^2} \lambda^{(\ell)} \right] \left(\frac{\sin \theta_c}{\cos \theta_c} \right). \quad (7.4)$$

These relations are free of neutral current parameters (c_R , c_I , θ_d) and can be inverted to determine the Cabibbo angle and the trace parameter:

$$\tan \theta_c = \frac{V_{us}^\ell - V_{cd}^\ell}{V_{ud}^\ell + V_{cs}^\ell}, \quad \frac{v^2}{\Lambda^2} \lambda^{(3,\ell)} \approx \frac{(V_{us}^\ell - V_{cd}^\ell)^2 + (V_{ud}^\ell + V_{cs}^\ell)^2 - 4}{8}. \quad (7.5)$$

Experimental information on V_{ij}^ℓ has to be extracted from lepton specific processes. We will impose as experimental constraints super-allowed β decay, charged pion, kaon, τ and charm decays. We detail the experimental inputs of charged-current processes and the extraction procedure in appendix A.

As for the high- p_T constraints, analogous expressions to eq. (6.1) hold for charged currents processes ($pp \rightarrow \ell\nu$) which bound the parameter space only in the $c^{(3)} = (c^{(-)} - c^{(+)})/2$ direction (see figure 5). Since the neutral current constraints allow for larger effects in $c^{(+)}$ than in $c^{(-)}$ the charged current constraints are relevant only for $c^{(+)}$.

8 Results

Our main results in terms of current experimental constraints on the $X^{(\pm)}$ components are summarized in eqs. (4.6) and (5.8) for the flavour universal CPV contributions, as well as in figures 3 and 4 for the CP conserving effects.

In figure 3 we present the combined fit to the most relevant experimental constraints on the $(-)$ operators with electrons (upper plot), muons (middle plot) and taus (lower plot). We observe that away from the down-quark mass basis alignment limit ($\theta_{\ell,d}^{(-)} \simeq 0$) the constraints are completely dominated by the NA62 measurement of $\mathcal{B}(K^+ \rightarrow \pi^+ \nu \bar{\nu})$ (marked with black dashed lines). Thus future planned improvements in this measurement [84] are

expected to have an important effect on all three lepton-specific operators. The nontrivial behavior of the (green shaded) 68% CL regions of the global fit is also due to the possible interferences between the SM and NP contributions to this decay. Interestingly, and as first pointed out in ref. [31], the constraints in the charm sector are currently dominated by Drell-Yan measurements at the LHC (marked with full black lines), with the exception of muonic operators, where the current best constraint is given by the LHCb upper bound on $\mathcal{B}(D^0 \rightarrow \mu^+ \mu^-)$ [20] (marked in black dotted line). In light of this, future improvements in the search for this rare decay by both LHCb and BelleII [85] are thus highly anticipated (projections shown in blue dotted line). For electron operators current bounds from high- p_T and rare $D \rightarrow \pi e^+ e^-$ measurements are comparable. Future measurements of the later decays by LHCb and BelleII, especially away from the long-distance resonance peaks in the $e^+ e^-$ invariant mass spectrum, could potentially improve this bound considerably. Finally, since all low energy decay channels for tauonic operators are closed, any future improvements in this sector will necessarily rely on precise (HL)LHC measurements of the $pp \rightarrow \tau\tau$ spectrum. Currently, the high- p_T experiments allow us to set a limit on the CP violating phase for the tau. The weakest derived bound at 95 % CL reads:

$$|\text{Im}[c_{\tau,I}^{(+)}]| \lesssim 0.15. \tag{8.1}$$

In figure 4 we present the combined fit to the most relevant experimental constraints on the (+) operators with electrons (upper plot), muons (middle plot) and taus (lower plot). In this case we observe that away from the down-quark mass basis alignment limit the constraints in the electron and muon sectors are dominated by $K_L \rightarrow \ell^+ \ell^-$ decay rate measurements (marked with dashed black lines). Therefore it is important that in the future, a combined analysis of $K^0 \rightarrow \ell\ell$ decays [74] could possibly go beyond the current sensitivity. Again high- p_T Drell-Yan production measurements (marked with black full lines) are most restrictive close to $\theta_{\ell,d}^{(+)} \simeq 0$. In the case of tauonic operators, LHC constraints dominate over the whole $\theta_{\tau,d}^{(+)}$ range. Interestingly, the almost flat behavior of these constraints with $\theta_{\ell,d}^{(+)}$ is a result of the non-trivial interplay between flavour changing ($\bar{s}d$ and $\bar{d}s$) and flavour conserving ($\bar{d}d$ and $\bar{s}s$) initial state contributions which exhibit opposite behavior, combined with the marginalization over the trace contributions ($\lambda^{(+)}$), see eq. (6.1).

To be competitive with the high- p_T constraints, the current experimental bound on $\mathcal{B}(D^0 \rightarrow \pi^0 \nu \bar{\nu})$ (not shown, see section 5.3) would have to be improved by 3 orders of magnitude. It is also important to note that at present, neutral current constraints are already stringent enough to make possible effects in charged current transitions negligible.

9 Conclusions

We considered the effects of BSM physics in rare semileptonic $\Delta C = 1$ and $\Delta S = 1$ processes mediated by purely left-handed quark and lepton operators. Restricting the discussion to the two light quark generations allowed us to parametrize possible BSM effects in quark flavour space in terms of Hermitian matrices (X) of dimension two, parametrized

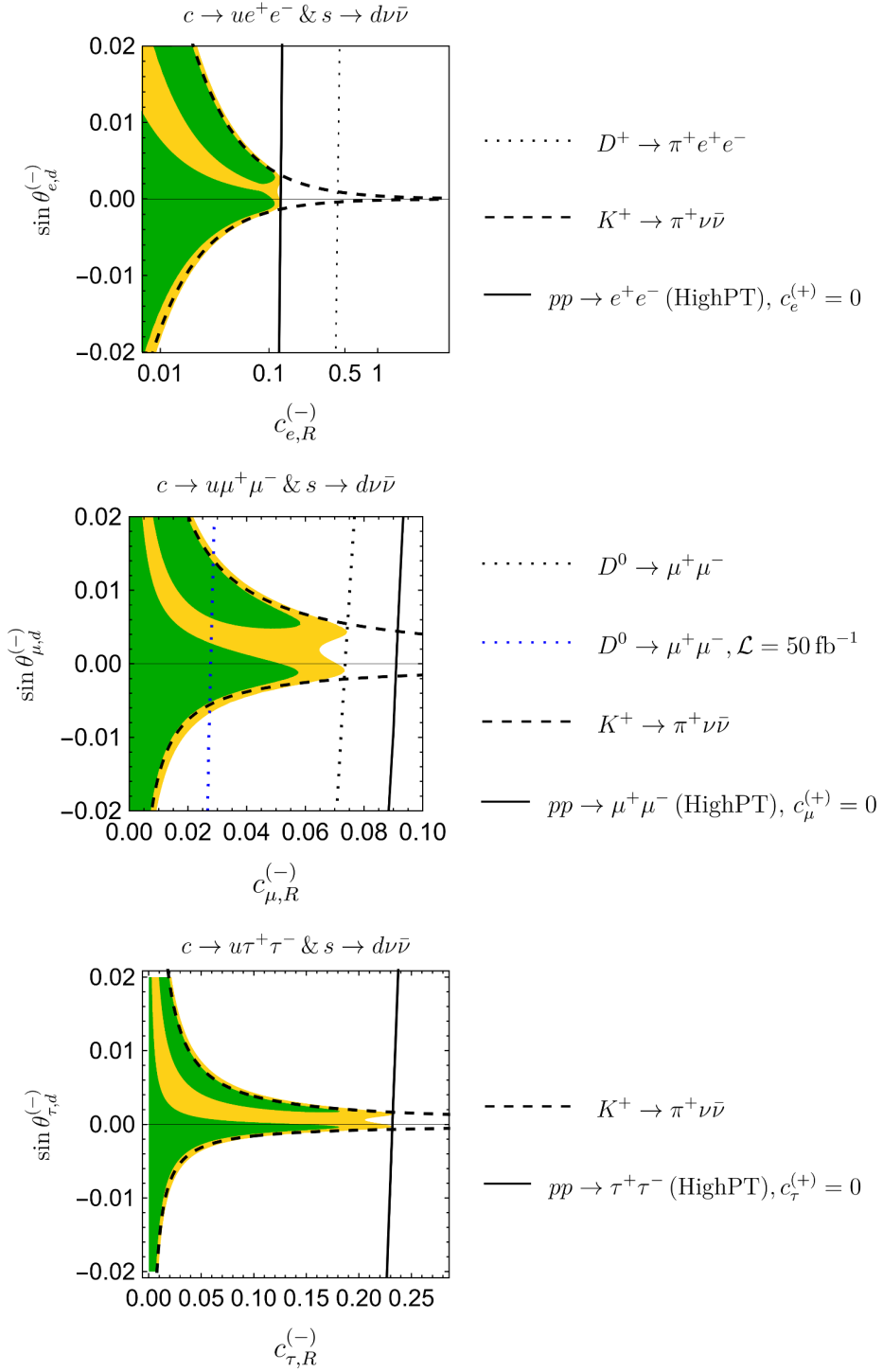


Figure 3. Bounds on the $(-)$ operators. The imaginary part (for all three lepton generations) was taken to be $c_{\ell,I}^{(-)} \simeq 0.4 \times 10^{-4}$, for which the bounds on $c_{\ell,R}^{(-)} \sin \theta_{\ell,d}^{(-)}$ from $K^+ \rightarrow \pi^+\nu\bar{\nu}$ are the weakest. The green and yellow shaded regions correspond to 68% CL and 95% CL allowed regions of the global fit. The HighPT bounds were derived under the assumption that $c_{\ell,R}^{(+)} = c_{\ell,I}^{(+)} = 0$.

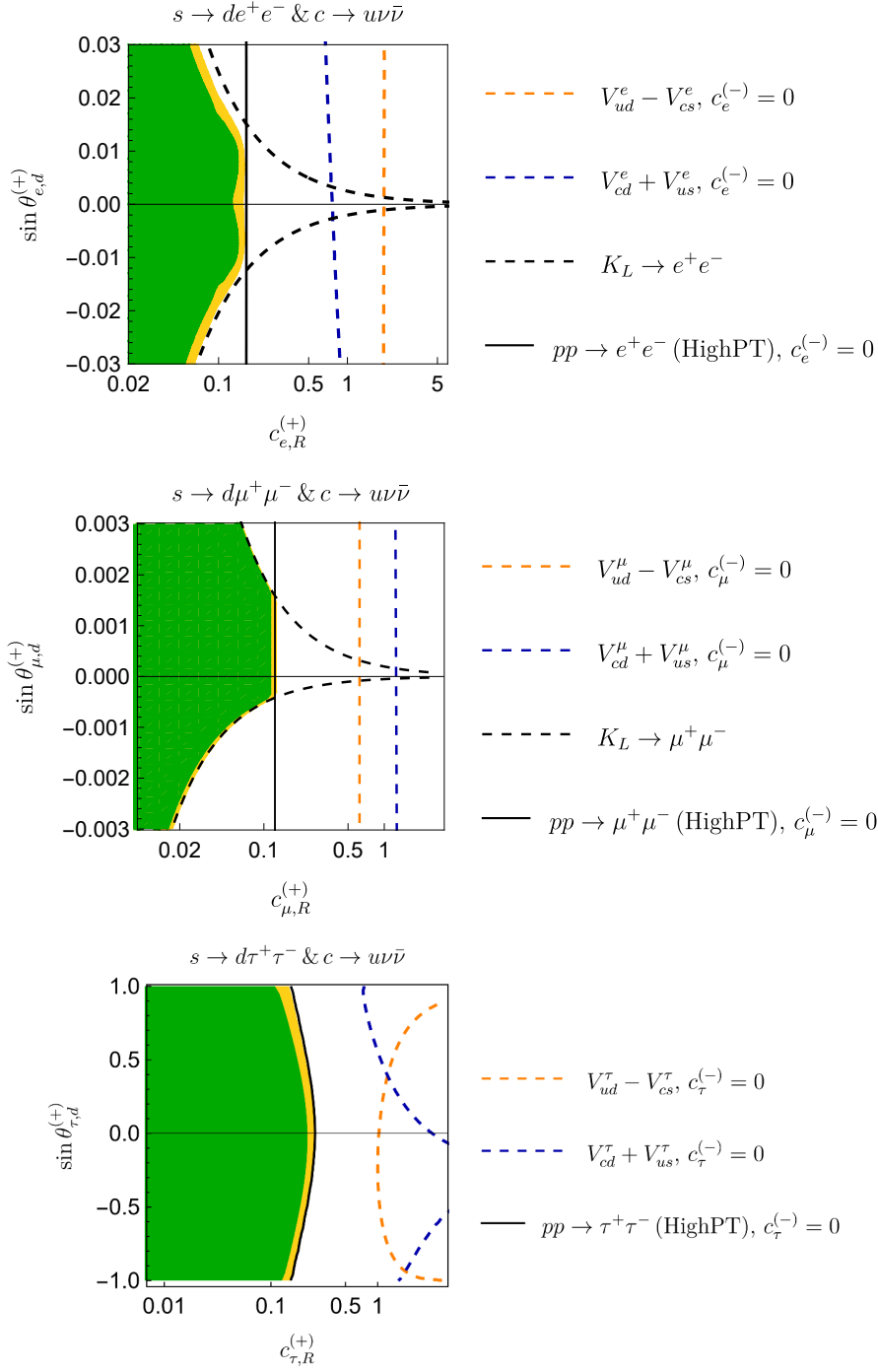


Figure 4. Constraints on $c_R^{(+)}$ and $\theta_d^{(+)}$ from various experimental bounds. Here we have set $c_{\ell,I}^{(+)}$ to zero. The green and yellow shaded regions correspond to 68% CL and 95% CL allowed regions of the global fit. The HighPT and charged current bounds were derived under the assumption that $c_{\ell,R}^{(-)} = c_{\ell,I}^{(-)} = 0$.

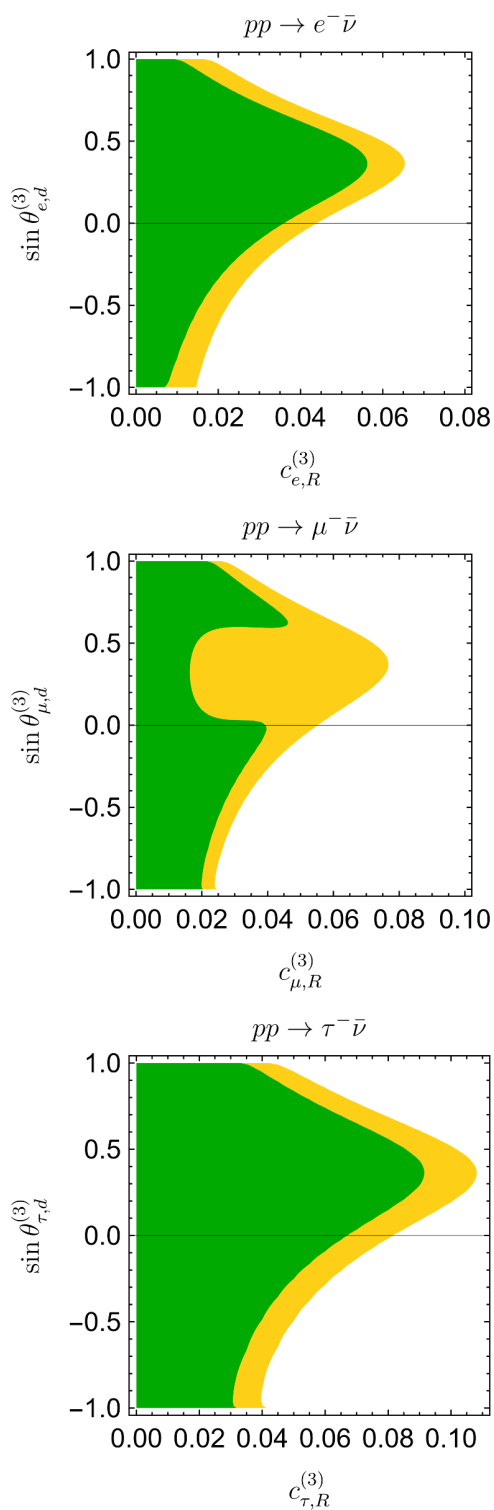


Figure 5. Bounds on the triplet operators from high- p_T charged current processes [47]. See text for details.

by three real and one imaginary coefficient. In addition, weak isospin singlet and triplet operator contributions are split into two distinct phenomenological sectors: one is characterized by effective BSM couplings $X^{(-)}$ and contributes to $s \rightarrow d\nu\bar{\nu}$ and $c \rightarrow ul^+\ell^-$ transitions. On the other hand $c \rightarrow uv\bar{\nu}$ and $s \rightarrow dl^+\ell^-$ processes can receive contributions from effective $X^{(+)}$ couplings. A distinct feature that emerges in such a framework is that beyond the SM there exists a single universal source of CP violation, parametrized by a single CP-violating coefficient for each ((-) and (+)) sector.

To determine the allowed parameter space, in the (-) sector we considered exclusive decays $D \rightarrow \pi\ell^+\ell^-$, $D \rightarrow \ell^+\ell^-$ and $K \rightarrow \pi\nu\bar{\nu}$. The $K_L \rightarrow \pi^-\nu\bar{\nu}$ decay amplitude is CP violating and the existing upper bound on the corresponding decay rate from KOTO directly constrains CPV in this sector. In practice however, the decay rate $K^+ \rightarrow \pi^+\nu\bar{\nu}$ is currently more sensitive and already constrains the CPV contribution in $X^{(-)}$ to below $\sim 10^{-4}$. The same CP-violating coefficient contributes also to charm meson decays. However, the lack of high-precision measurements in rare charm semileptonic decays currently precludes any competitive CPV probes in this sector. In the $X^{(+)}$ sector, the decay modes $K_L \rightarrow \pi^0\ell^+\ell^-$ and $K_L \rightarrow \ell^+\ell^-$ dominate the low energy constraints.

Importantly, low energy data from exclusive K and D decays is complemented by constraints from high- p_T processes $pp \rightarrow \ell^+\ell^-$ at the LHC. In the case of electrons, these bounds are currently competitive with the existing data on the rates of $D^+ \rightarrow \pi^+e^+e^-$ (for $X^{(-)}$) and $K_L \rightarrow e^+e^-$ (for $X^{(+)}$). They also dominate the constraints in the $X^{(+)}$ sector for tau leptons. Interestingly, flavour conserving and flavour changing neutral currents contribute to $pp \rightarrow \ell^+\ell^-$ in a complementary way, allowing to completely constrain both $X^{(\pm)}$ parameter spaces using only high- p_T data.

The presence of weak isospin triplet operators in the effective Lagrangian implies that charged current processes might receive BSM contributions as well. Therefore, our analysis considered constraints from super-allowed beta decays, from (semi)leptonic kaon decays used in the extraction of the CKM matrix element V_{us} , as well as from charged current-induced (semi)leptonic decays of charmed mesons. We found that these constraints are more pronounced in the $X^{(+)}$ sector, where they currently supersede the ones coming from the FCNC process $D \rightarrow \pi\nu\nu$. They are however not competitive with high- p_T constraints.

In the future, improved bounds on BSM physics entering D and K rare semileptonic decays are expected from high precision measurements of both charm decay rates ($D^+ \rightarrow \pi^+\ell^+\ell^-$, $D \rightarrow \ell^+\ell^-$ and $D \rightarrow \pi\nu\bar{\nu}$), as well as kaon decay rates ($K^+ \rightarrow \pi^+\nu\bar{\nu}$, $K_L \rightarrow \pi^0\nu\bar{\nu}$ and $K^0 \rightarrow \mu^+\mu^-$). At the same time, future precision measurements of high p_T processes $pp \rightarrow \ell^+\ell^-$ at (HL)LHC, especially in the tau sector, could further illuminate and constrain possible BSM physics in strange and charm semileptonic processes.

Acknowledgments

J.F.K. is grateful to the Mainz Institute for Theoretical Physics (MITP) of the Cluster of Excellence PRISMA⁺ (Project ID 39083149), for its hospitality and its partial support during the completion of this work. We acknowledge the financial support from the Slovenian Research Agency (research core funding No. P1-0035 and J1-3013).

A Lepton-specific CKM elements

The lepton-specific modifications of the CKM elements of eq. (7.1) are:

$$\begin{aligned}
 (\Lambda^2/v^2)\Delta V_{ud}^{(\ell)} &= +\lambda^{(3,\ell)} \cos \theta_c - \frac{1}{2}c_R^{(+)} \cos(\theta_c + \theta_d^{(+)}) + \frac{1}{2}c_R^{(-)} \cos(\theta_c + \theta_d^{(-)}) \\
 &\quad + \frac{i}{2} \sin \theta_c (c_I^{(+)} - c_I^{(-)}), \tag{A.1a}
 \end{aligned}$$

$$\begin{aligned}
 (\Lambda^2/v^2)\Delta V_{us}^{(\ell)} &= +\lambda^{(3,\ell)} \sin \theta_c + \frac{1}{2}c_R^{(+)} \sin(\theta_c + \theta_d^{(+)}) - \frac{1}{2}c_R^{(-)} \sin(\theta_c + \theta_d^{(-)}) \\
 &\quad - \frac{i}{2} \cos \theta_c (c_I^{(+)} - c_I^{(-)}), \tag{A.1b}
 \end{aligned}$$

$$\begin{aligned}
 (\Lambda^2/v^2)\Delta V_{cd}^{(\ell)} &= -\lambda^{(3,\ell)} \sin \theta_c + \frac{1}{2}c_R^{(+)} \sin(\theta_c + \theta_d^{(+)}) - \frac{1}{2}c_R^{(-)} \sin(\theta_c + \theta_d^{(-)}) \\
 &\quad + \frac{i}{2} \cos \theta_c (c_I^{(+)} - c_I^{(-)}), \tag{A.1c}
 \end{aligned}$$

$$\begin{aligned}
 (\Lambda^2/v^2)\Delta V_{cs}^{(\ell)} &= +\lambda^{(3,\ell)} \cos \theta_c + \frac{1}{2}c_R^{(+)} \cos(\theta_c + \theta_d^{(+)}) - \frac{1}{2}c_R^{(-)} \cos(\theta_c + \theta_d^{(-)}) \\
 &\quad - \frac{i}{2} \sin \theta_c (c_I^{(+)} - c_I^{(-)}), \tag{A.1d}
 \end{aligned}$$

As we do not assume lepton flavour universality, it is necessary to extract constraints separately for each lepton flavour.

A.1 V_{ud}^ℓ

For electrons, we use the measured value of the superallowed β decay, which limits the parameter space in the direction of C_{ud}^e . Using the results presented in [39, 86], and the derived matching conditions, we have:

$$\begin{aligned}
 |V_{ud}^e|^2 &= \left| V_{ud} + \frac{v^2}{\Lambda^2} \left(\lambda^{(3,e)} \cos \theta_c - \frac{1}{2}c_R^{(+)} \cos(\theta_c + \theta_d^{(+)}) + \frac{1}{2}c_R^{(-)} \cos(\theta_c + \theta_d^{(-)}) \right) \right|^2 \\
 &= \frac{2984.432(3)s}{\mathcal{F}t(1 + \Delta_R^V)} \tag{A.2}
 \end{aligned}$$

where $\mathcal{F}t = 3072(2)s$ and $\Delta_R^V = 0.02426(32)$ [87].⁵

In order to limit this CKM element for muons and taus, we use the following LFU ratio [89]:

$$R_{\tau/\mu}^\pi = \frac{\Gamma(\tau^- \rightarrow \pi^- \nu_\tau)}{\Gamma(\pi^- \rightarrow \mu^- \nu_\mu)} = \left(\frac{V_{ud}^\tau}{V_{ud}^\mu} \right)^2 \frac{m_\tau^3}{2m_\pi m_\mu^2} \frac{(1 - m_\pi^2/m_\tau^2)^2}{(1 - m_\mu^2/m_\pi^2)} (1 + \delta R_{\tau/\mu}^\pi), \tag{A.3}$$

where $\delta R_{\tau/\mu}^\pi = (0.16 \pm 0.14)\%$ is the ratio of radiative corrections [90]. When deriving limits, we consider only one lepton-specific contribution at a time, while keeping the other CKM element fixed at the SM value.

The theoretical prediction can be compared to the ratio of measured decays:

$$R_{\tau/\mu}^{\pi(\text{exp})} = 0.9962 \pm 0.0027. \tag{A.4}$$

⁵Other measurements for these values exist as well, see e.g. [88]. We choose the ones with larger uncertainties.

A.2 V_{us}^ℓ

We employ the precisely determined LFU ratios in kaon decays, namely:

$$R_{e/\mu}^K = \frac{\Gamma(K^- \rightarrow e^- \bar{\nu})}{\Gamma(K^- \rightarrow \mu^- \bar{\nu})}, \quad (\text{A.5})$$

$$R_{\tau/\mu}^K = \frac{\Gamma(\tau^- \rightarrow K^- \nu)}{\Gamma(K^- \rightarrow \mu^- \bar{\nu})}, \quad (\text{A.6})$$

and adapt the same approach as previously. The ratio in eq. (A.5) is used in our fits to limit V_{us}^e and V_{us}^μ , whereas eq. (A.6) is used to limit V_{us}^τ . In case NP is present only in electrons, the experimental value in eq. (A.5) can be compared to our theoretical prediction:

$$\frac{R_{e/\mu}^{K(\text{exp})}}{R_{e/\mu}^{K(\text{SM})}} - 1 \approx \frac{v^2}{\Lambda^2} \left[c_R^{(+)} \sin(\theta_d^{(+)} + \theta_c) - c_R^{(-)} \sin(\theta_d^{(-)} + \theta_c) + 2\lambda^{(3,e)} \sin \theta_c \right] / \sin \theta_c, \quad (\text{A.7})$$

with similar expressions for the other two lepton generations. Here:

$$R_{e/\mu}^{K(\text{exp})} = (2.488 \pm 0.010) \times 10^{-5}, \quad R_{e/\mu}^{K(\text{SM})} = (2.477 \pm 0.001) \times 10^{-5}. \quad (\text{A.8})$$

A.3 V_{cd}^ℓ and V_{cs}^ℓ

HFLAV [91] gives world-average lepton-specific measurements (bounds) on $V_{cd}^{\mu,\tau}$ and $V_{cs}^{\mu,\tau}$ from the branching ratios $D^+ \rightarrow \ell^+ \nu$ and $D_s^+ \rightarrow \ell^+ \nu$. As the bounds on electron-specific coefficients V_{cd}^e, V_{cs}^e are very weak, we use other charm decays instead, in particular $D \rightarrow \pi^- e^+ \nu$ and $D \rightarrow K^- e^+ \nu$, for which the NP-dependent branching ratios read:

$$\begin{aligned} \frac{d\mathcal{B}}{dq^2}(D^0 \rightarrow P e^+ \nu) = \\ \frac{G_F^2 |V_{cq'}^e|^2}{384 m_D^3 \pi^3 \Gamma_D} \left(1 - \frac{m_e^2}{q^2}\right)^2 \sqrt{\lambda} \left(f_{+D \rightarrow P}^2(q^2) \left(2 + \frac{m_e^2}{q^2}\right) \lambda + 3 f_{0D \rightarrow P}^2(q^2) \frac{m_e^2}{q^2} (m_D^2 - m_P^2)^2 \right). \end{aligned} \quad (\text{A.9})$$

Here $\lambda \equiv \lambda(m_D^2, m_P^2, q^2)$ and $P = \pi^-$ ($q' = d$) or K^- ($q' = s$). The momentum transfer squared can take values in the range $m_e^2 \leq q^2 \leq (m_D - m_P)^2$. We can compare the integrated branching ratios with the experimental values:

$$\begin{aligned} \mathcal{B}^{(\text{exp})}(D^0 \rightarrow \pi^- e^+ \nu) &= (2.91 \pm 0.04) \times 10^{-3}, \\ \mathcal{B}^{(\text{exp})}(D^0 \rightarrow K^- e^+ \nu) &= (3.549 \pm 0.026) \times 10^{-2}. \end{aligned} \quad (\text{A.10})$$

A.4 Limits

We summarize our results in the table 3.

	CKM Element	Measurement/Experiment	Derived value
e	V_{ud}^e	Superaligned β decay	0.9736 ± 0.0002
	V_{us}^e	$R_{e/\mu}^K$ (NP in e)	0.2255 ± 0.0004
	V_{cd}^e	$D^0 \rightarrow \pi^- e^+ \nu$	-0.235 ± 0.008
	V_{cs}^e	$D^0 \rightarrow K^- e^+ \nu$	0.98 ± 0.04
μ	V_{ud}^μ	$R_{\tau/\mu}^\pi$ (NP in μ)	0.9781 ± 0.0027
	V_{us}^μ	$R_{e/\mu}^K$ (NP in μ)	0.2245 ± 0.0005
	V_{cd}^μ	$D^+ \rightarrow \mu^+ \nu$ (HFLAV)	-0.225 ± 0.007
	V_{cs}^μ	$D_s^+ \rightarrow \mu^+ \nu$ (HFLAV)	0.97 ± 0.02
τ	V_{ud}^τ	$R_{\tau/\mu}^\pi$ (NP in τ)	0.9707 ± 0.0026
	V_{us}^τ	$R_{\tau/\mu}^K$ (NP in τ)	0.222 ± 0.002
	V_{cd}^τ	$D^+ \rightarrow \tau^+ \nu$ (HFLAV)	-0.25 ± 0.03
	V_{cs}^τ	$D_s^+ \rightarrow \tau^+ \nu$ (HFLAV)	0.98 ± 0.02

Table 3. Experimental input used to limit the lepton-specific CKM contributions.

Open Access. This article is distributed under the terms of the Creative Commons Attribution License ([CC-BY 4.0](https://creativecommons.org/licenses/by/4.0/)), which permits any use, distribution and reproduction in any medium, provided the original author(s) and source are credited.

References

- [1] S. Bifani, S. Descotes-Genon, A. Romero Vidal and M.-H. Schune, *Review of Lepton Universality tests in B decays*, *J. Phys. G* **46** (2019) 023001 [[arXiv:1809.06229](https://arxiv.org/abs/1809.06229)] [[INSPIRE](#)].
- [2] M. Artuso, G. Isidori and S. Stone, *New Physics in b Decays*, World Scientific (2022) [[DOI:10.1142/12696](https://doi.org/10.1142/12696)] [[INSPIRE](#)].
- [3] D. Buttazzo, A. Greljo, G. Isidori and D. Marzocca, *B-physics anomalies: a guide to combined explanations*, *JHEP* **11** (2017) 044 [[arXiv:1706.07808](https://arxiv.org/abs/1706.07808)] [[INSPIRE](#)].
- [4] C. Cornella, J. Fuentes-Martin and G. Isidori, *Revisiting the vector leptoquark explanation of the B-physics anomalies*, *JHEP* **07** (2019) 168 [[arXiv:1903.11517](https://arxiv.org/abs/1903.11517)] [[INSPIRE](#)].
- [5] R. Barbieri, C. Cornella and G. Isidori, *Simplified models of vector SU(4) leptoquarks at the TeV*, *Eur. Phys. J. C* **82** (2022) 1161 [[arXiv:2207.14248](https://arxiv.org/abs/2207.14248)] [[INSPIRE](#)].
- [6] A. Angelescu et al., *Single leptoquark solutions to the B-physics anomalies*, *Phys. Rev. D* **104** (2021) 055017 [[arXiv:2103.12504](https://arxiv.org/abs/2103.12504)] [[INSPIRE](#)].
- [7] I. Doršner, S. Fajfer, D.A. Faroughy and N. Košnik, *The role of the S₃ GUT leptoquark in flavor universality and collider searches*, *JHEP* **10** (2017) 188 [[arXiv:1706.07779](https://arxiv.org/abs/1706.07779)] [[INSPIRE](#)].
- [8] D. Bečirević et al., *Scalar leptoquarks from grand unified theories to accommodate the B-physics anomalies*, *Phys. Rev. D* **98** (2018) 055003 [[arXiv:1806.05689](https://arxiv.org/abs/1806.05689)] [[INSPIRE](#)].
- [9] D. Bečirević et al., *Model with two scalar leptoquarks: R2 and S3*, *Phys. Rev. D* **106** (2022) 075023 [[arXiv:2206.09717](https://arxiv.org/abs/2206.09717)] [[INSPIRE](#)].

- [10] A. Crivellin, D. Müller and T. Ota, *Simultaneous explanation of $R(D^{(*)})$ and $b \rightarrow s\mu^+ \mu^-$: the last scalar leptoquarks standing*, *JHEP* **09** (2017) 040 [[arXiv:1703.09226](#)] [[INSPIRE](#)].
- [11] J. Aebischer, A.J. Buras and J. Kumar, *On the Importance of Rare Kaon Decays: A Snowmass 2021 White Paper*, in the proceedings of the *2021 Snowmass Summer Study*, (2022) [[arXiv:2203.09524](#)] [[INSPIRE](#)].
- [12] A.J. Buras, *On the Standard Model Predictions for Rare K and B Decay Branching Ratios: 2022*, [arXiv:2205.01118](#) [[INSPIRE](#)].
- [13] S. Fajfer and N. Košnik, *Prospects of discovering new physics in rare charm decays*, *Eur. Phys. J. C* **75** (2015) 567 [[arXiv:1510.00965](#)] [[INSPIRE](#)].
- [14] S. De Boer and G. Hiller, *Null tests from angular distributions in $D \rightarrow P_1 P_2 l^+ l^-$, $l = e, \mu$ decays on and off peak*, *Phys. Rev. D* **98** (2018) 035041 [[arXiv:1805.08516](#)] [[INSPIRE](#)].
- [15] R. Bause, H. Gisbert, M. Golz and G. Hiller, *Rare charm $c \rightarrow u \nu \bar{\nu}$ dineutrino null tests for $e^+ e^-$ machines*, *Phys. Rev. D* **103** (2021) 015033 [[arXiv:2010.02225](#)] [[INSPIRE](#)].
- [16] R. Bause, H. Gisbert, M. Golz and G. Hiller, *Lepton universality and lepton flavor conservation tests with dineutrino modes*, *Eur. Phys. J. C* **82** (2022) 164 [[arXiv:2007.05001](#)] [[INSPIRE](#)].
- [17] G. Faisel, J.-Y. Su and J. Tandean, *Exploring charm decays with missing energy in leptoquark models*, *JHEP* **04** (2021) 246 [[arXiv:2012.15847](#)] [[INSPIRE](#)].
- [18] R. Bause, H. Gisbert, M. Golz and G. Hiller, *Interplay of dineutrino modes with semileptonic rare B-decays*, *JHEP* **12** (2021) 061 [[arXiv:2109.01675](#)] [[INSPIRE](#)].
- [19] J.F. Kamenik, A. Katz and D. Stolarski, *On Lepton Flavor Universality in Top Quark Decays*, *JHEP* **01** (2019) 032 [[arXiv:1808.00964](#)] [[INSPIRE](#)].
- [20] LHCb collaboration, *Search for rare decays of D^0 mesons into two muons*, [arXiv:2212.11203](#) [[INSPIRE](#)].
- [21] LHCb collaboration, *Searches for 25 rare and forbidden decays of D^+ and D_s^+ mesons*, *JHEP* **06** (2021) 044 [[arXiv:2011.00217](#)] [[INSPIRE](#)].
- [22] BESIII collaboration, *Search for the decay $D^0 \rightarrow \pi^0 \nu \bar{\nu}$* , *Phys. Rev. D* **105** (2022) L071102 [[arXiv:2112.14236](#)] [[INSPIRE](#)].
- [23] NA62 collaboration, *Measurement of the very rare $K^+ \rightarrow \pi^+ \nu \bar{\nu}$ decay*, *JHEP* **06** (2021) 093 [[arXiv:2103.15389](#)] [[INSPIRE](#)].
- [24] NA62 collaboration, *A measurement of the $K^+ \rightarrow \pi^+ \mu^+ \mu^-$ decay*, *JHEP* **11** (2022) 011 [*Addendum ibid.* **06** (2023) 040] [[arXiv:2209.05076](#)] [[INSPIRE](#)].
- [25] KOTO collaboration, *Study of the $K_L \rightarrow \pi^0 \nu \bar{\nu}$ Decay at the J-PARC KOTO Experiment*, *Phys. Rev. Lett.* **126** (2021) 121801 [[arXiv:2012.07571](#)] [[INSPIRE](#)].
- [26] R.K. Ellis et al., *Physics Briefing Book: Input for the European Strategy for Particle Physics Update 2020*, [arXiv:1910.11775](#) [[INSPIRE](#)].
- [27] O. Gedalia, J.F. Kamenik, Z. Ligeti and G. Perez, *On the Universality of CP Violation in $\Delta F = 1$ Processes*, *Phys. Lett. B* **714** (2012) 55 [[arXiv:1202.5038](#)] [[INSPIRE](#)].
- [28] K. Blum, Y. Grossman, Y. Nir and G. Perez, *Combining K^0 - anti- K^0 mixing and D^0 - anti- D^0 mixing to constrain the flavor structure of new physics*, *Phys. Rev. Lett.* **102** (2009) 211802 [[arXiv:0903.2118](#)] [[INSPIRE](#)].

- [29] O. Gedalia, L. Mannelli and G. Perez, *Covariant Description of Flavor Violation at the LHC*, *Phys. Lett. B* **693** (2010) 301 [[arXiv:1002.0778](#)] [[INSPIRE](#)].
- [30] O. Gedalia, L. Mannelli and G. Perez, *Covariant Description of Flavor Conversion at the LHC Era*, *JHEP* **10** (2010) 046 [[arXiv:1003.3869](#)] [[INSPIRE](#)].
- [31] J. Fuentes-Martin, A. Greljo, J. Martin Camalich and J.D. Ruiz-Alvarez, *Charm physics confronts high- p_T lepton tails*, *JHEP* **11** (2020) 080 [[arXiv:2003.12421](#)] [[INSPIRE](#)].
- [32] L. Allwicher et al., *Drell-Yan tails beyond the Standard Model*, *JHEP* **03** (2023) 064 [[arXiv:2207.10714](#)] [[INSPIRE](#)].
- [33] A. Greljo, J. Salko, A. Smolkovič and P. Stangl, *Rare b decays meet high-mass Drell-Yan*, *JHEP* **05** (2023) 087 [[arXiv:2212.10497](#)] [[INSPIRE](#)].
- [34] B. Grzadkowski, M. Iskrzynski, M. Misiak and J. Rosiek, *Dimension-Six Terms in the Standard Model Lagrangian*, *JHEP* **10** (2010) 085 [[arXiv:1008.4884](#)] [[INSPIRE](#)].
- [35] ALEPH et al. collaborations, *Precision electroweak measurements on the Z resonance*, *Phys. Rept.* **427** (2006) 257 [[hep-ex/0509008](#)] [[INSPIRE](#)].
- [36] OPAL collaboration, *Measurement of the $e^+e^- \rightarrow W^+W^-$ cross section and W decay branching fractions at LEP*, *Eur. Phys. J. C* **52** (2007) 767 [[arXiv:0708.1311](#)] [[INSPIRE](#)].
- [37] PARTICLE DATA GROUP collaboration, *Review of Particle Physics*, *PTEP* **2022** (2022) 083C01 [[INSPIRE](#)].
- [38] A.M. Coutinho, A. Crivellin and C.A. Manzari, *Global Fit to Modified Neutrino Couplings and the Cabibbo-Angle Anomaly*, *Phys. Rev. Lett.* **125** (2020) 071802 [[arXiv:1912.08823](#)] [[INSPIRE](#)].
- [39] A. Crivellin and M. Hoferichter, *β Decays as Sensitive Probes of Lepton Flavor Universality*, *Phys. Rev. Lett.* **125** (2020) 111801 [[arXiv:2002.07184](#)] [[INSPIRE](#)].
- [40] M. Kirk, *Cabibbo anomaly versus electroweak precision tests: An exploration of extensions of the Standard Model*, *Phys. Rev. D* **103** (2021) 035004 [[arXiv:2008.03261](#)] [[INSPIRE](#)].
- [41] A. Crivellin, M. Kirk, T. Kitahara and F. Mescia, *Global fit of modified quark couplings to EW gauge bosons and vector-like quarks in light of the Cabibbo angle anomaly*, *JHEP* **03** (2023) 234 [[arXiv:2212.06862](#)] [[INSPIRE](#)].
- [42] G. D'Ambrosio, G.F. Giudice, G. Isidori and A. Strumia, *Minimal flavor violation: An Effective field theory approach*, *Nucl. Phys. B* **645** (2002) 155 [[hep-ph/0207036](#)] [[INSPIRE](#)].
- [43] E.E. Jenkins, A.V. Manohar and M. Trott, *Renormalization Group Evolution of the Standard Model Dimension Six Operators II: Yukawa Dependence*, *JHEP* **01** (2014) 035 [[arXiv:1310.4838](#)] [[INSPIRE](#)].
- [44] E949 collaboration, *New measurement of the $K^+ \rightarrow \pi^+ \nu \bar{\nu}$ branching ratio*, *Phys. Rev. Lett.* **101** (2008) 191802 [[arXiv:0808.2459](#)] [[INSPIRE](#)].
- [45] BELLE collaboration, *Search for leptonic decays of D^0 mesons*, *Phys. Rev. D* **81** (2010) 091102 [[arXiv:1003.2345](#)] [[INSPIRE](#)].
- [46] LHCb collaboration, *Search for $D_s^+ \rightarrow \pi^+ \mu^+ \mu^-$ and $D_s^+ \rightarrow \pi^- \mu^+ \mu^+$ decays*, *Phys. Lett. B* **724** (2013) 203 [[arXiv:1304.6365](#)] [[INSPIRE](#)].
- [47] L. Allwicher et al., *HighPT: A tool for high- p_T Drell-Yan tails beyond the standard model*, *Comput. Phys. Commun.* **289** (2023) 108749 [[arXiv:2207.10756](#)] [[INSPIRE](#)].

- [48] J. Brod, M. Gorbahn and E. Stamou, *Updated Standard Model Prediction for $K \rightarrow \pi\nu\bar{\nu}$ and ϵ_K* , *PoS BEAUTY2020* (2021) 056 [[arXiv:2105.02868](#)] [[INSPIRE](#)].
- [49] A.J. Buras and E. Venturini, *The exclusive vision of rare K and B decays and of the quark mixing in the standard model*, *Eur. Phys. J. C* **82** (2022) 615 [[arXiv:2203.11960](#)] [[INSPIRE](#)].
- [50] A.J. Buras, *Standard Model predictions for rare K and B decays without new physics infection*, *Eur. Phys. J. C* **83** (2023) 66 [[arXiv:2209.03968](#)] [[INSPIRE](#)].
- [51] A.J. Buras and E. Venturini, *Searching for New Physics in Rare K and B Decays without $|V_{cb}|$ and $|V_{ub}|$ Uncertainties*, *Acta Phys. Polon. B* **53** (2021) A1 [[arXiv:2109.11032](#)] [[INSPIRE](#)].
- [52] A.J. Buras, D. Buttazzo, J. Girrbach-Noe and R. Knegjens, *$K^+ \rightarrow \pi^+\nu\bar{\nu}$ and $K_L \rightarrow \pi^0\nu\bar{\nu}$ in the Standard Model: status and perspectives*, *JHEP* **11** (2015) 033 [[arXiv:1503.02693](#)] [[INSPIRE](#)].
- [53] F. Mescia and C. Smith, *Improved estimates of rare K decay matrix-elements from $Kl3$ decays*, *Phys. Rev. D* **76** (2007) 034017 [[arXiv:0705.2025](#)] [[INSPIRE](#)].
- [54] A.J. Buras, M. Gorbahn, U. Haisch and U. Nierste, *The Rare decay $K^+ \rightarrow \pi^+\nu\bar{\nu}$ at the next-to-next-to-leading order in QCD*, *Phys. Rev. Lett.* **95** (2005) 261805 [[hep-ph/0508165](#)] [[INSPIRE](#)].
- [55] A.J. Buras, M. Gorbahn, U. Haisch and U. Nierste, *Charm quark contribution to $K^+ \rightarrow \pi^+\nu\bar{\nu}$ at next-to-next-to-leading order*, *JHEP* **11** (2006) 002 [Erratum *ibid.* **11** (2012) 167] [[hep-ph/0603079](#)] [[INSPIRE](#)].
- [56] ETM collaboration, *$K \rightarrow \pi\ell\nu$ Semileptonic Form Factors from Two-Flavor Lattice QCD*, *Phys. Rev. D* **80** (2009) 111502 [[arXiv:0906.4728](#)] [[INSPIRE](#)].
- [57] S. Fajfer, *Long distance contribution to $K^+ \rightarrow \pi^+\nu\bar{\nu}$ neutrino anti-neutrino decay and $O(p^4)$ terms in CHPT*, *Nuovo Cim. A* **110** (1997) 397 [[hep-ph/9602322](#)] [[INSPIRE](#)].
- [58] G. Isidori, F. Mescia and C. Smith, *Light-quark loops in $K^+ \rightarrow \pi^+\nu\bar{\nu}$ anti-nu*, *Nucl. Phys. B* **718** (2005) 319 [[hep-ph/0503107](#)] [[INSPIRE](#)].
- [59] KOTO collaboration, *Search for the $K_L \rightarrow \pi^0\nu\bar{\nu}$ and $K_L \rightarrow \pi^0X^0$ decays at the J-PARC KOTO experiment*, *Phys. Rev. Lett.* **122** (2019) 021802 [[arXiv:1810.09655](#)] [[INSPIRE](#)].
- [60] G. Burdman, E. Golowich, J.A.L. Hewett and S. Pakvasa, *Rare charm decays in the standard model and beyond*, *Phys. Rev. D* **66** (2002) 014009 [[hep-ph/0112235](#)] [[INSPIRE](#)].
- [61] BELLE collaboration, *Search for the rare decay $D^0 \rightarrow \gamma\gamma$ at Belle*, *Phys. Rev. D* **93** (2016) 051102 [[arXiv:1512.02992](#)] [[INSPIRE](#)].
- [62] A. Paul, I.I. Bigi and S. Recksiegel, *$D^{0-} \rightarrow \gamma\gamma$ and $D^{0-} \rightarrow \mu^+\mu^-$ Rates on an Unlikely Impact of the Littlest Higgs Model with T-Parity*, *Phys. Rev. D* **82** (2010) 094006 [Erratum *ibid.* **83** (2011) 019901] [[arXiv:1008.3141](#)] [[INSPIRE](#)].
- [63] R. Bause, M. Golz, G. Hiller and A. Tayduganov, *The new physics reach of null tests with $D \rightarrow \pi\ell\ell$ and $D_s \rightarrow K\ell\ell$ decays*, *Eur. Phys. J. C* **80** (2020) 65 [Erratum *ibid.* **81** (2021) 219] [[arXiv:1909.11108](#)] [[INSPIRE](#)].
- [64] BNL E871 collaboration, *First observation of the rare decay mode $K0(L) \rightarrow e^+e^-$* , *Phys. Rev. Lett.* **81** (1998) 4309 [[hep-ex/9810007](#)] [[INSPIRE](#)].
- [65] E871 collaboration, *Improved branching ratio measurement for the decay $K0(L) \rightarrow \mu^+\mu^-$* , *Phys. Rev. Lett.* **84** (2000) 1389 [[INSPIRE](#)].

- [66] KTEV collaboration, *Search for the Decay $K_L \rightarrow \pi^0 \mu^+ \mu^-$* , *Phys. Rev. Lett.* **84** (2000) 5279 [[hep-ex/0001006](#)] [[INSPIRE](#)].
- [67] G. D'Ambrosio, G. Ecker, G. Isidori and J. Portoles, *The Decays $K \rightarrow \pi \ell^+ \ell^-$ beyond leading order in the chiral expansion*, *JHEP* **08** (1998) 004 [[hep-ph/9808289](#)] [[INSPIRE](#)].
- [68] G. Buchalla, G. D'Ambrosio and G. Isidori, *Extracting short distance physics from $K(L,S) \rightarrow \pi^0 e^+ e^-$ decays*, *Nucl. Phys. B* **672** (2003) 387 [[hep-ph/0308008](#)] [[INSPIRE](#)].
- [69] G. Isidori, C. Smith and R. Unterdorfer, *The Rare decay $K_L \rightarrow \pi^0 \mu^+ \mu^-$ within the SM*, *Eur. Phys. J. C* **36** (2004) 57 [[hep-ph/0404127](#)] [[INSPIRE](#)].
- [70] F. Mescia, C. Smith and S. Trine, *$K(L) \rightarrow \pi^0 e^+ e^-$ and $K(L) \rightarrow \mu^0 e^+ \mu^-$: A Binary star on the stage of flavor physics*, *JHEP* **08** (2006) 088 [[hep-ph/0606081](#)] [[INSPIRE](#)].
- [71] G. Buchalla, A.J. Buras and M.E. Lautenbacher, *Weak decays beyond leading logarithms*, *Rev. Mod. Phys.* **68** (1996) 1125 [[hep-ph/9512380](#)] [[INSPIRE](#)].
- [72] NA48/1 collaboration, *Observation of the rare decay $K(S) \rightarrow \pi^0 e^+ e^-$* , *Phys. Lett. B* **576** (2003) 43 [[hep-ex/0309075](#)] [[INSPIRE](#)].
- [73] L.-S. Geng, J.M. Camalich and R.-X. Shi, *New physics in $s \rightarrow d$ semileptonic transitions: rare hyperon vs. kaon decays*, *JHEP* **02** (2022) 178 [[arXiv:2112.11979](#)] [[INSPIRE](#)].
- [74] A. Dery, M. Ghosh, Y. Grossman and S. Schacht, *$K \rightarrow \mu^+ \mu^-$ as a clean probe of short-distance physics*, *JHEP* **07** (2021) 103 [[arXiv:2104.06427](#)] [[INSPIRE](#)].
- [75] FLAVOUR LATTICE AVERAGING GROUP (FLAG) collaboration, *FLAG Review 2021*, *Eur. Phys. J. C* **82** (2022) 869 [[arXiv:2111.09849](#)] [[INSPIRE](#)].
- [76] G. Isidori and R. Unterdorfer, *On the short distance constraints from $K(L,S) \rightarrow \mu^+ \mu^-$* , *JHEP* **01** (2004) 009 [[hep-ph/0311084](#)] [[INSPIRE](#)].
- [77] J.-M. Gerard, C. Smith and S. Trine, *Radiative kaon decays and the penguin contribution to the Delta $I = 1/2$ rule*, *Nucl. Phys. B* **730** (2005) 1 [[hep-ph/0508189](#)] [[INSPIRE](#)].
- [78] G. Valencia, *Long distance contribution to $K(L) \rightarrow \text{lepton}^+ \text{lepton}^-$* , *Nucl. Phys. B* **517** (1998) 339 [[hep-ph/9711377](#)] [[INSPIRE](#)].
- [79] P. Colangelo, F. De Fazio and F. Loporco, *$c \rightarrow u \nu \nu^-$ transitions of Bc mesons: 331 model facing Standard Model null tests*, *Phys. Rev. D* **104** (2021) 115024 [[arXiv:2107.07291](#)] [[INSPIRE](#)].
- [80] ETM collaboration, *Scalar and vector form factors of $D \rightarrow \pi(K) \ell \nu$ decays with $N_f = 2 + 1 + 1$ twisted fermions*, *Phys. Rev. D* **96** (2017) 054514 [Erratum *ibid.* **99** (2019) 099902] [[arXiv:1706.03017](#)] [[INSPIRE](#)].
- [81] A. Greljo and D. Marzocca, *High- p_T dilepton tails and flavor physics*, *Eur. Phys. J. C* **77** (2017) 548 [[arXiv:1704.09015](#)] [[INSPIRE](#)].
- [82] ATLAS collaboration, *Search for heavy Higgs bosons decaying into two tau leptons with the ATLAS detector using pp collisions at $\sqrt{s} = 13$ TeV*, *Phys. Rev. Lett.* **125** (2020) 051801 [[arXiv:2002.12223](#)] [[INSPIRE](#)].
- [83] CMS collaboration, *Search for resonant and nonresonant new phenomena in high-mass dilepton final states at $\sqrt{s} = 13$ TeV*, *JHEP* **07** (2021) 208 [[arXiv:2103.02708](#)] [[INSPIRE](#)].
- [84] E. Goudzovski et al., *New physics searches at kaon and hyperon factories*, *Rept. Prog. Phys.* **86** (2023) 016201 [[arXiv:2201.07805](#)] [[INSPIRE](#)].

- [85] BELLE-II collaboration, *The Belle II Physics Book*, *PTEP* **2019** (2019) 123C01 [Erratum *ibid.* **2020** (2020) 029201] [[arXiv:1808.10567](#)] [[INSPIRE](#)].
- [86] J.C. Hardy and I.S. Towner, *Superaligned $0^+ \rightarrow 0^+$ nuclear β decays: 2014 critical survey, with precise results for V_{ud} and CKM unitarity*, *Phys. Rev. C* **91** (2015) 025501 [[arXiv:1411.5987](#)] [[INSPIRE](#)].
- [87] A. Czarnecki, W.J. Marciano and A. Sirlin, *Radiative Corrections to Neutron and Nuclear Beta Decays Revisited*, *Phys. Rev. D* **100** (2019) 073008 [[arXiv:1907.06737](#)] [[INSPIRE](#)].
- [88] C.-Y. Seng, M. Gorchtein, H.H. Patel and M.J. Ramsey-Musolf, *Reduced Hadronic Uncertainty in the Determination of V_{ud}* , *Phys. Rev. Lett.* **121** (2018) 241804 [[arXiv:1807.10197](#)] [[INSPIRE](#)].
- [89] A. Pich, *Precision Tau Physics*, *Prog. Part. Nucl. Phys.* **75** (2014) 41 [[arXiv:1310.7922](#)] [[INSPIRE](#)].
- [90] W.J. Marciano and A. Sirlin, *Radiative corrections to $\pi(\text{lepton } 2)$ decays*, *Phys. Rev. Lett.* **71** (1993) 3629 [[INSPIRE](#)].
- [91] HEAVY FLAVOR AVERAGING GROUP and HFLAV collaborations, *Averages of b -hadron, c -hadron, and τ -lepton properties as of 2021*, *Phys. Rev. D* **107** (2023) 052008 [[arXiv:2206.07501](#)] [[INSPIRE](#)].